PERGAMON

Journal of Structural Geology 23 (2001) 455–472

JOURNAL OF STRUCTURAL GEOLOGY

www.elsevier.nl/locate/jstrugeo

# Stress and deformation patterns in the Aegean region

Theodor Doutsos*, Sotiris Kokkalas

*Department of Geology, University of Patras, 26500 Patras, Greece*

Received 18 June 2000; accepted 23 July 2000

**Abstract**

The Aegean region constitutes the overriding plate of the Africa–Eurasia convergent plate system, in the eastern Mediterranean. To explain the fault kinematics and tectonic forces that controlled rift evolution in the Aegean area, we present fault-slip data from about 900 faults, and summarise the structural analyses of five key structural "provinces". Five regional tectonic maps are used as the basis for a new stress map for the Aegean region and for discussions on regional geodynamics.

Since the Late Miocene, the central Aegean has been affected by WNW- and NE-trending faults which transfer the motion of the Anatolian plate to the southwest, synchronous with arc-normal pull acting on the boundary of the Aegean plate. At the same time, the Hellenic Peninsula has suffered moderate extension by NW-trending grabens formed due to collapse of the Hellenic mountain chain.

During intense extension in the southern Aegean in the Plio-Quaternary the arcuate shape of the Hellenic Trench was established. Arc-normal pull in the Aegean plate margin, combined with transform resistive forces along the Hellenic subduction gave rise to widespread strike-slip and oblique-normal faults in the eastern segment and moderate oblique extension in the western segment of the arc. To the north, subduction involves more continental crust and consequently the push of subduction is transmitted to the overriding plate (Hellenic Peninsula), resulting in the formation of NE-trending grabens. WNW-trending grabens in this area are considered to have propagated westward from the Aegean Sea to the Ionian Sea during Plio-Quaternary times, probably acting as pull-apart structures between stable Europe and the rapidly extending southern Aegean area. 

## 1. Introduction

In the Aegean area, intense and widely distributed extension started in Serravalian time (Drooger and Meulenkamp, 1973; Le Pichon and Angelier, 1979) and remains ongoing (McKenzie, 1972; Papazachos et al., 1984; Jackson et al., 1992) as it is suggested by seismic studies and strain rates estimated by GPS measurements (Billiris et al., 1991; Davies et al., 1997; Kahle et al., 1998). On the Hellenic Peninsula most of this extension is accommodated along a series of large-scale normal faults, which reach a depth of 8–12 km (Jackson et al., 1982; Doutsos and Poulimenos 1992). Maximum extension ($\beta = 1.8$, Angelier et al., 1982) occurs in the Cretan Sea region where the crust is thinner than 20 km (Makris, 1978; McKenzie, 1978). The crust has been previously thickened during the collision of several microplates, which completed in the Early Miocene (Jacobshagen, 1986; Doutsos et al., 1993).

Extension is genetically related to two first-order structures: the North Anatolian transform fault (NAF) and the Hellenic subduction zone (McKenzie, 1972; Dewey and Celal Sengor, 1979; Le Pichon et al., 1980; Fig. 1). The Aegean–Anatolian microplate is driven westward between the North Anatolian (NAF) and East Anatolian (EAF) transform faults (Fig. 1, inset) in response to the northward collision of the Arabian plate into the Eurasian plate. In the western part of this microplate, the Aegean back-arc basin is confined to the south by the Hellenic Trench, along which the oceanic part of the African plate is consumed northwards. It is an open question today which part of the observed extension is related to movements transmitted to the Aegean area along the NAF, and which one is related to the roll-back of the Hellenic subduction. Most interpretations emphasize the role of the westward push of the Anatolian plate (Jackson, 1994; Taymaz et al., 1991; Le Pichon et al., 1995), whereas others highlight the role of subduction roll-back and trench suction of the area north of the Hellenic Trench, which represents a "free edge boundary" (Le Pichon and Angelier 1979; Hatzfeld et al., 1997; Meijer and Wortel, 1997). Another group of authors have attributed most extensional structures in Peloponnese and Kythira to resistive forces associated with convergence along the subduction interface (Lyon-Caen et al., 1988; Mercier et al., 1989; Armijo and Lyon-Caen, 1992).

Stress data derived by fault-slip analysis in the classic

* Corresponding author. Tel.: +30-61-997-841; Fax: +30-61-994-485.
*E-mail address:* tdoutsos@upatras.gr (T. Doutsos).

0191-8141/01/$ - see front matter 
PII: S0191-8141(00)00119-X

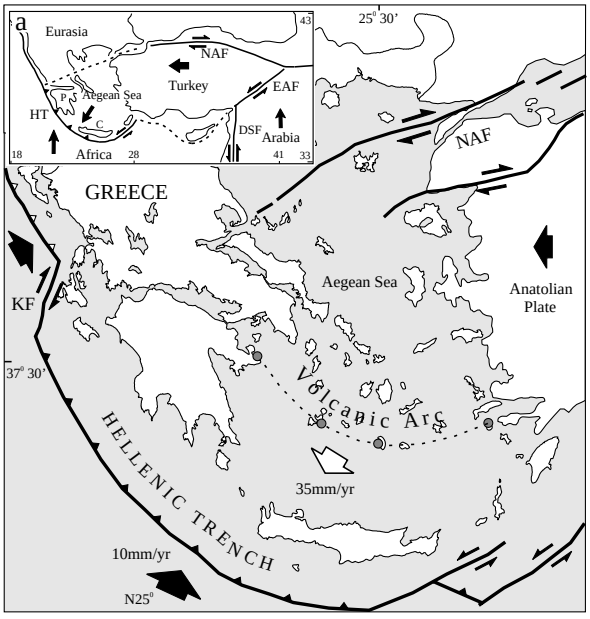


Fig. 1. General map showing the main structural features of the Hellenic Arc and Trench system. Motion vectors of the African plate and the Aegean microplate after Kahle et al. (1998). KF = Kefallonia Fault, NAF = North Anatonian Fault. Inset a: Schematic map summarizing the geodynamic framework around the eastern Mediterranean Sea together with the major plates involved in collision process (after McKenzie, 1972). NAF = North Anatolian Fault, EAF = East Anatolian Fault, DSF = Dead Sea Fault, HT = Hellenic Trench, P = Peloponnesus, C = Crete.

papers of Angelier et al. (1982) and Mercier et al. (1989) show a variability which does not explain the driving mechanisms for the extension. Although both papers present similar stress data regarding the Plio-Quaternary evolution of the southern Aegean and support the radial spreading of this region toward the Hellenic Arc, they present different stress data for the Hellenic Peninsula and suggest a change in extension direction up to 70° within the Quaternary. However, such changes may represent local stress deviations from a regional stress and therefore are not caused by changes of the plate tectonic forces. Recent studies in the Central Greece question this change in the regional stress field and consider the stress field to be inhomogenous (Roberts, 1996; Roberts and Ganas, in press). Slip-vectors, along basin forming faults and surface ruptures of single earthquakes, converge toward the center of the fault surface where the maximum displacements are observed (Jackson et al., 1982; Roberts and Koukouvelas, 1996). It is thought likely that some slip patterns presented in earlier studies have been measured from the end of the faults and therefore do not represent the direction of regional extension. In many cases local stress is a dependent variable arisen from displacements along intersecting normal faults (Scott et al., 1994; Maerten et al., 1999) or from displacements along major, often pre-existing, faults (Sylvester, 1988; Tikoff and Wojtal, 1999). It is likely that the multidirectional fault pattern described by Angelier (1979) in the Aegean area and the oblique subduction on the southeastern part of the Hellenic trench promotes such local stress changes in the area. Furthermore, we note that in the stress maps of Angelier et al. (1982) and Mercier et al. (1989) there is a lack of Plio-Quaternary stress data for several areas, such as NW Greece, NW Peloponessus and the Cycladic islands; for Late Miocene times, stress data are missing from the Hellenic Peninsula and the southern Aegean area.

In order to fill these gaps and construct a new stress map for the Aegean area, we analyze fault-slip data on about 900 faults, most of which are taken from the center of large mappable faults within post-Middle Miocene basins. Subsequently we distinguish (*sensu* Zoback and Zoback, 1991) five stress provinces, each of which is characterized by consistent local stress and deformation. Finally, to describe kinematics and construct a dynamic model for the Aegean motion we discuss for each one stress province appropriate mechanisms to explain local stress and deformation.

## 2. Methods of fault-slip data

The fault-slip data have been collected from basin-bounding faults, as well as along large faults within the Late Miocene to recent extensional basins. These data correspond to measurements of striations and other sense of slip indicators, determined using criteria summarized by Hancock (1985) and Petit (1987).

We have analyzed fault-slip data by both the graphical and numerical methods for palaeostress analysis. The graphical methods include the P–T axes method (Turner, 1953) and the right dihedra method (Angelier and Mechler, 1977). The numerical analysis includes the direct inversion (Angelier and Goguel, 1979) and the numerical dynamic analysis (Spang, 1972). The results from the numerical methods serve as a check and add to the accuracy of the results. Basic assumptions and limitations of palaeostress analysis techniques were discussed by Etchecopar et al. (1981), Reches (1987), Marrett and Allmendinger (1990) and Angelier (1994) among others. Major requirements are coaxial deformation and a homogenous stress field throughout each station.

Fortunately, many of the numerical procedures for stress inversion contain internal checks on these assumptions. These checks involve comparisons of the measured striation directions with those predicted on the basis of the computed stresses. Furthermore, the degree of spatial homogeneity can be evaluated for a given data set by analyzing subgroups of faults and comparing their kinematics. Comparing the fault kinematics at the different measurement sites in the study area indicates that kinematics are spatially homogenous (see also Marrett and Allmendinger, 1990). In addition, because slip-vectors can vary along faults (Roberts, 1996), we report fault-slip data close to the centre of all the faults in a given area in order to constrain regionally significant extension directions.

Table 1
Palaeostress tensors from fault-slip data; n = number of fault data used; $\delta_1$, $\delta_2$, and $\delta_3$ = azimuth and plunge of principal stress axes; $R$ = stress ratio $(\delta_2 - \delta_3)/(\delta_1 - \delta_3)$; $F$ = mean slip deviation; SR = stress regime; m = Late Miocene; pq = Plio-Quaternary

| Site | Age | Location | $n$ | $\delta_1$ | $\delta_2$ | $\delta_3$ | $R$ | $F$ | SR |
|---|---|---|---|---|---|---|---|---|---|
| | | A.1. Stress tensors for the stress province A | | | | | | | |
| SPA1 | pq | Ptolemaida basin | 46 | 152/85 | 250/01 | 340/05 | 0.48 | 0.35 | normal |
| SPA2 | m | Mesohellenic Trough | 21 | 330/70 | 215/05 | 120/03 | 0.32 | 0.28 | normal |
| SPA3 | m | Mesohellenic Trough | 8 | 355/68 | 140/18 | 232/10 | 0.12 | 0.32 | radial tension |
| | | A.2. Stress tensors for the stress province B | | | | | | | |
| Site | Age | Location | $n$ | $\delta_1$ | $\delta_2$ | $\delta_3$ | $R$ | $F$ | SR |
| SPB1 | pq | Rio graben | 34 | 341/86 | 86/01 | 176/04 | 0.46 | 0.25 | normal |
| SPB2 | pq | West Corinth graben | 23 | 126/85 | 284/05 | 14/02 | 0.37 | 0.19 | normal |
| SPB3 | pq | Abelon graben | 17 | 171/84 | 57/02 | 326/05 | 0.05 | 0.13 | radial tension |
| SPB4 | pq | Pyrgos graben | 27 | 227/85 | 99/03 | 09/04 | 0.27 | 0.24 | normal |
| SPB5 | pq | Nedas graben | 15 | 108/59 | 311/29 | 215/10 | 0.51 | 0.37 | normal |
| SPB6 | pq | Corinth area | 30 | 95/87 | 249/03 | 339/01 | 0.47 | 0.22 | normal |
| SPB7 | pq | Corinth area | 10 | 223/79 | 109/05 | 18/10 | 0.45 | 0.22 | normal |
| SPB8 | pq | Corinth area | 38 | 108/84 | 249/05 | 339/04 | 0.44 | 0.23 | normal |
| SPB9 | pq | Atalanti graben | 10 | 344/76 | 91/04 | 182/13 | 0.28 | 0.27 | normal |
| SPB10 | m | North Evia | 27 | 354/56 | 158/33 | 253/08 | 0.63 | 0.33 | normal/strike-slip |
| SPB11 | m | Kymi basin | 44 | 358/76 | 158/13 | 249/05 | 0.34 | 0.35 | normal |
| | | A.3. Stress tensors for the stress province C | | | | | | | |
| Site | Age | Location | $n$ | $\delta_1$ | $\delta_2$ | $\delta_3$ | $R$ | $F$ | SR |
| SPC1 | pq | Kalamata graben | 21 | 341/75 | 167/15 | 77/01 | 0.27 | 0.30 | normal |
| SPC2 | m–pq | Kythira island | 6 | 350/72 | 114/11 | 207/15 | 0.56 | 0.34 | normal |
| SPC3 | pq | Kythira island | 8 | 203/76 | 355/12 | 87/06 | 0.29 | 0.22 | normal |
| SPC4 | pq | Antikythira island | 6 | 198/79 | 359/10 | 90/03 | 0.57 | 0.28 | normal |
| SPC5 | m–pq | Gramvusa peninsula | 7 | 165/60 | 04/29 | 269/08 | 0.48 | 0.34 | normal |
| | | A.4. Stress tensors for the stress province D | | | | | | | |
| Site | Age | Location | $n$ | $\delta_1$ | $\delta_2$ | $\delta_3$ | $R$ | $F$ | SR |
| SPD1 | m | Paros | 6 | 280/42 | 109/48 | 14/05 | 0.18 | 0.22 | strike-slip |
| SPD2 | m | Naxos | 15 | 99/1 | 170/62 | 09/28 | 0.54 | 0.25 | pure strike-slip |
| SPD3 | pq | Ikaria | 13 | 142/57 | 297/31 | 34/11 | 0.98 | 0.15 | normal/strike-slip |
| SPD4 | m | Koufonisia | 12 | 159/05 | 36/81 | 250/05 | 0.84 | 0.22 | strike-slip/normal |
| SPD5 | m | Samos | 22 | 82/20 | 263/65 | 351/03 | 0.44 | 0.24 | strike-slip |
| SPD6 | pq | Kos | 6 | 194/78 | 297/03 | 28/12 | 0.33 | 0.35 | normal |
| SPD7 | m | Kos | 10 | 72/28 | 289/56 | 171/17 | 0.6 | 0.18 | strike-slip/normal |
| SPD8 | m | Anafi | 15 | 351/61 | 123/20 | 221/20 | 0.02 | 0.15 | radial tension |
| SPD9 | m–pq | Rethimno | 8 | 155/70 | 55/04 | 324/20 | 0.4 | 0.13 | normal |
| SPD10 | pq | Paleochora | 5 | 41/04 | 304/56 | 134/34 | 0.68 | 0.39 | strike-slip/normal |
| SPD11 | m–pq | Episkopi r.z. | 14 | 348/66 | 143/25 | 237/03 | 0.59 | 0.29 | normal/strike-slip |
| SPD12 | m–pq | Episkopi r.z. | 18 | 289/65 | 198/02 | 108/25 | 0.47 | 0.45 | normal |
| SPD13 | m–pq | Topolia basin | 9 | 73/63 | 288/23 | 192/14 | 0.55 | 0.02 | normal |
| SPD14 | m–pq | Episkopi r.z. | 15 | 242/81 | 147/01 | 57/09 | 0.48 | 0.39 | normal |
| SPD15 | m–pq | Topolia basin | 15 | 135/82 | 141/07 | 250/03 | 0.40 | 0.56 | normal |
| SPD16 | m | Milos | 9 | 132/33 | 264/46 | 24/26 | 0.70 | 0.10 | strike-slip/normal |
| | | A.5. Stress tensors for the stress province E | | | | | | | |
| Site | Age | Location | $n$ | $\delta_1$ | $\delta_2$ | $\delta_3$ | $R$ | $F$ | SR |
| SPE1 | m | Ierapetra basin | 29 | 150/81 | 283/06 | 13/07 | 0.46 | 0.06 | normal |
| SPE2 | m | Ierapetra basin | 16 | 76/69 | 236/20 | 329/07 | 0.71 | 0.1 | normal/strike-slip |
| SPE3 | pq | East Ierapetra basin | 36 | 25/78 | 202/32 | 87/01 | 0.1 | 0.19 | radial tension |
| SPE4 | pq | Ierapetra basin | 9 | 358/37 | 197/51 | 95/09 | 0.6 | 0.08 | strike-slip/normal |
| SPE5 | m | Fothia basin | 16 | 76/69 | 236/20 | 329/07 | 0.71 | 0.10 | normal/strike-slip |
| SPE6 | pq | Sitia graben | 20 | 27/70 | 202/20 | 292/01 | 0.44 | 0.12 | normal |
| SPE7 | pq | Sitia graben | 23 | 249/77 | 50/12 | 140/04 | 0.68 | 0.14 | normal/strike-slip |
| SPE8 | pq | Sitia graben (south) | 22 | 72/83 | 208/05 | 298/05 | 0.41 | 0.13 | normal |
| SPE9 | m | Kasos island | 9 | 69/70 | 314/08 | 222/18 | 0.27 | 0.44 | normal |
| SPE10 | pq | Kasos island | 12 | 351/47 | 175/43 | 83/02 | 0.5 | 0.13 | normal |
| SPE11 | pq | South Karpathos | 6 | 135/74 | 270/12 | 02/11 | 0.72 | 0.32 | normal/strike-slip |
| SPE12 | pq | West Karpathos | 10 | 09/38 | 202/52 | 104/06 | 0.6 | 0.29 | strike-slip/normal |
| SPE13 | pq | South Karpathos | 6 | 259/81 | 23/05 | 114/08 | 0.53 | 0.3 | normal |
| SPE14 | pq | East Karpathos | 13 | 287/13 | 42/65 | 193/21 | 0.81 | 0.22 | strike-slip/normal |
| SPE15 | pq | Rhodes island | 13 | 67/81 | 202/06 | 293/06 | 0.47 | 0.38 | normal |
| SPE16 | pq | Rhodes island | 22 | 294/83 | 180/03 | 90/06 | 0.52 | 0.31 | normal |

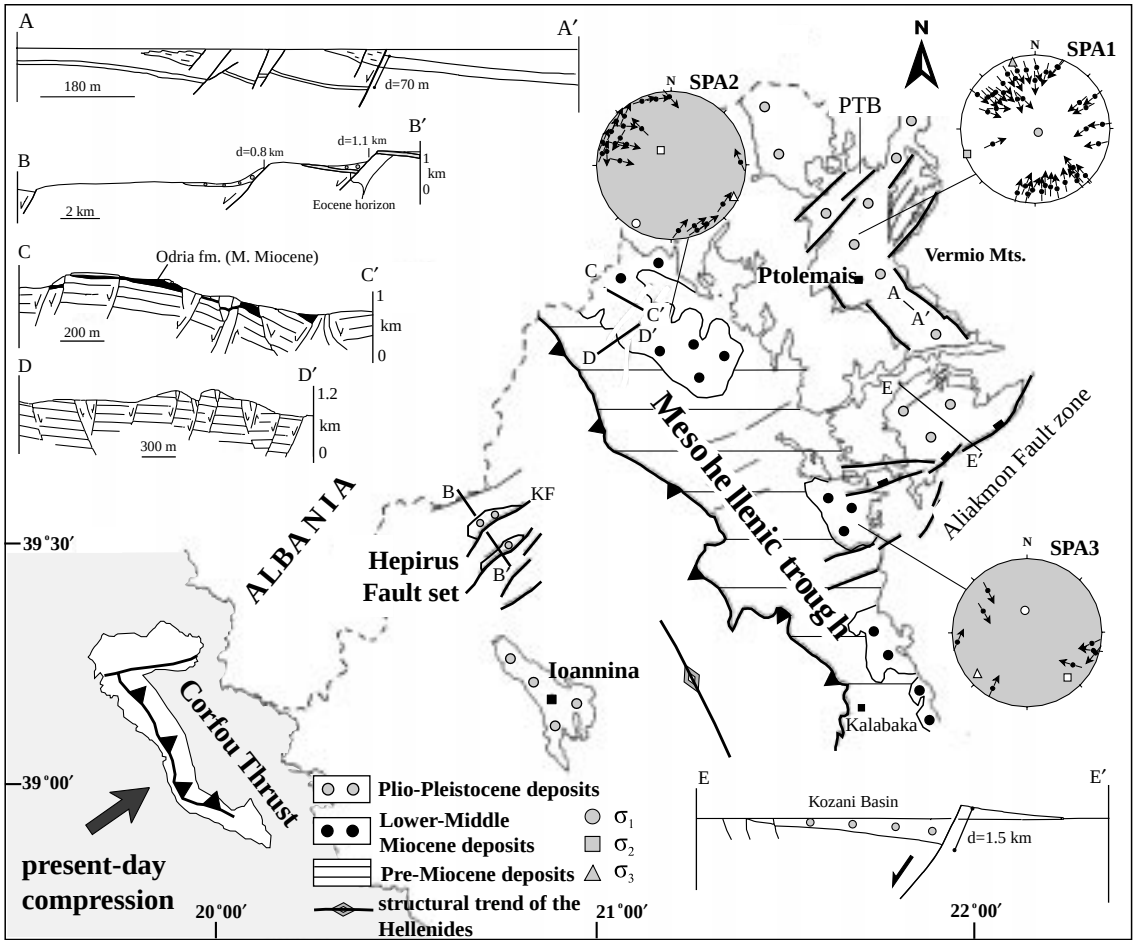


Fig. 2. Simplified map of the northwestern Aegean area (stress province A). Stereonets with white coloring are related to the Plio-Quaternary evolution. Stereonets with uniform grey shading are related to the Late Miocene evolution. PTB = Ptolemais basin, KB = Kozani basin, KF = Konitsa fault. For station names refer to Table 1.

Application of methods lead to the determination of the reduced stress tensor, defined by the orientation of the three principal stress axes—$\delta_1$ (maximum compression), $\delta_2$ (intermediate compression), $\delta_3$ (minimum compression)—and the shape of stress ellipsoid ($R = [\delta_2 - \delta_3]/[\delta_1 - \delta_3]$). Parameter F defines the average deviation angle between the calculated theoretical striation and the actual striation of a fault-slip data set, for all calculated stress tensors, and helps to evaluate the homogeneity of data. In general, results with average angle lower than 20° ($F \leq 0.35$) were considered to be satisfactory.

To overcome the difficulties posed by the complex dynamic histories of the rocks studied and to isolate the effects of different stress tensors, our stress analysis took into consideration all the field observations, such as consistent fault superposition, synsedimentary faults, covered structures and relative age of fault striations, in order to assign the subsets to relative age groups. Chronostratigraphical constraints for the deformed rocks are given for each stress province separately.

The data are presented in equal-area, lower hemisphere stereonets with fault planes shown as poles and striae as arrows onto the poles, indicating the sense of movement of the hanging wall block (Hoeppener, 1955). The results of palaeostress determination are presented in Table 1 and on the map of Fig. 7a.

## 3. The northwestern Aegean area (Stress province A)

The northwestern Aegean area includes the northern part of the Hellenic mountain chain from the Hepirus region in the west to the Thermaikos Gulf in the east (Fig. 2). Stress patterns deduced from fault-slip data were given only for the easternmost part of this area, where Pavlides and Mountrakis (1987) proposed a change in the tension direction from NE–SW in the Late Miocene to NW–SE in the Pleistocene. Mercier et al. (1989) suggested a change in the $\delta_3$ orientation from NE during the Pliocene–Lower Pleistocene to NW from the Middle Pleistocene to the Quaternary. We

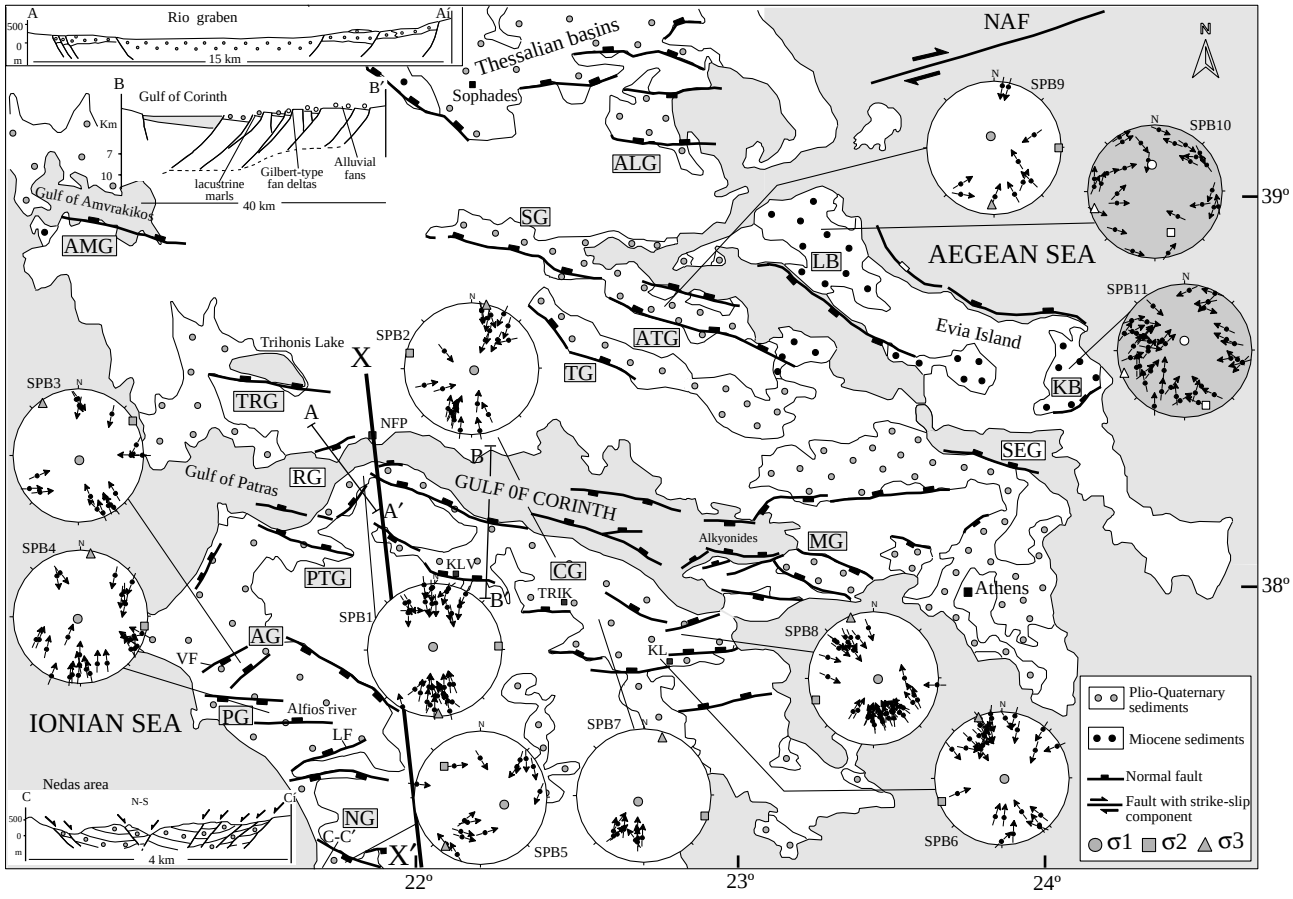


Fig. 3. Simplified map of the central Hellenic Peninsula (stress province B). Coloring of stereonets as in Fig. 2. AG = Abelon graben, ALG = Almyros graben, AMG = Amvrakikos graben, ATG = Atalanti graben, CG = Corinth graben, KB = Kymi basin, LB = Limni basin, MG = Megara graben, NG = Nedas graben, PG = Pyrgos graben, PTG = Patras graben, RG = Rio graben, SG = Sperhios graben, SEG = South Evoikos graben, TG = Tithorea graben, TRG = Trihonis graben, VF = Vounargos fault, LF = Lapithas Fault, KLV = Kalavrita village, TRIK = Trikala village, KL = Klenia village, NFP = Nafpaktos town.

accept that the two-phase extensional model is appropriate for the whole NW Aegean area, but we propose different chronological constraints.

### 3.1. Plio-Quaternary evolution

We recognize two first-order structures: the Hepiros fault set in the west and the Aliakmon fault zone in the east.

The Hepiros fault set comprises two NE-trending asymmetric grabens typically spaced 8–10 km apart (Fig. 2, cross-section B–B′). Recent movements along the master faults of these grabens are documented by the impressive fault scarp morphology of the area and by the young surficial deposits, which are concentrated in narrow zones along the faults. We estimated these movements by using Eocene limestones as a marker horizon (Fig. 2, cross-section B–B′). At the central part of the faults, maximum downthrow movements attain 1000 m and footwall uplift is of the order of 400 m. This uplift contributed significantly to the high topographic relief of the area. The Konitsa Fault (KF) is likely to be responsible for the 1996 ($M_L = 5.6$) Konitsa earthquake, which destroyed the southern part of the Konitsa village (Doutsos and Koukouvelas, 1998).

The 70-km-long, NE-trending Aliakmon fault zone is marked by large well-preserved scarps associated with lacustrine, colluvial and alluvial deposits of Middle Pleistocene to Holocene age. These deposits make up the upper part of a 600-m-southward thickening sedimentary wedge (Fig. 2, cross-section D–D′), which began to form in Middle Pliocene time (Brunn, 1956; Koufos et al., 1991). The height of the fault escarpment across the 45° dipping fault surface is 900 m, giving a cumulative displacement of 1500 m. A 25-km-long segment of this fault was activated during the 1995 ($M_L = 6.6$) Kozani–Grevena earthquake, which produced coseismic slip at the Earth's surface, of about 20 cm (Pavlides et al., 1995) and maximum coseismic slip of 0.5 m, at a depth of 10 km (Papazachos et al., 1995).

Furthermore, a conjugate system of nearly NE–SW trending normal faults has internally deformed the sedimentary fill of the Ptolemais basin (Fig. 2, stereonet $SPA_1$, cross-section A–A′). Kinematic parameters on reverse drag profiles, such as displacement, wavelength of hanging wall rollover, footwall uplift, wavelength of footwall uplift have

been estimated (Fig. 2, cross-section A–A′; Doutsos and Koukouvelas, 1998). Most of these faults have strongly affected the thickness of lignit horizons dated in the early Pliocene (Schneider and Velitzelos, 1973; Van de Weerd, 1979). These Early Pliocene faults are compatible with a roughly NW direction of $\delta_3$.

### 3.2. Late Miocene evolution

Northwest-striking normal faults controlled the early stages of formation of the Ptolemais basin (Pavlides and Mountrakis, 1987) and caused the deposition of a Late Miocene conglomerate-sandstone sequence (Gregor and Velitzelos, 1995). Further west within the Mesohellenic Trough, NW-trending normal faults (Fig. 2, cross-section D–D′) have strongly rotated the youngest molassic series, the Odria and Orlia series of Middle to Late Miocene age (Brunn, 1956; Doutsos et al., 1994). Another set of smaller NE-trending faults have affected these deposits (Fig. 2, cross-section C–C′). The computed $s_1$ axis is subvertical, the $\delta_2$ axis trends NW, parallel to the trend of the Pindos mountain chain and the $\delta_3$ axis trends NE (Fig. 2, stereonet $SPA_3$). In some places where NE-trending normal faults prevailed (Fig. 2, stereonet $SPA_2$) the $\delta_1$ axis remains constant, whereas $\delta_2$ and $\delta_3$ axes have similar magnitudes. This indicates that the direction of extension can easily vary.

### 3.3. Summary

We recognize that rift structures in the northwestern Aegean area were formed under moderate extension caused by a stress regime which changed with time: during the Late Miocene the minimum principal stress ($\delta_3$) is oriented NE, whereas $\delta_3$ has a NW orientation during the Plio-Quaternary.

## 4. The central Hellenic peninsula (stress province B)

The central Hellenic Peninsula represents the classic "basin-and-range"-type extensional area in Greece. Angelier et al. (1982) and Mercier et al. (1989) presented fault-slip data for this area and claimed a change in the $\delta_3$ orientation from NNE–SSW in the Pliocene to NNW–SSE in the present time. Roberts (1996) and Roberts and Ganas (in press) described a fault set of NE to WNW-trending faults, in the eastern Corinth graben, which formed under a constant direction of extension at 353°, during the last 2 Ma. Below, we present structural data to support (1) the argument that NE and WNW-trending faults are independent extensional structures which can locally interact, and (2) that a change in the style of extension took place at the Miocene/Pliocene boundary.

### 4.1. Plio-Quaternary evolution

Based on the amount of the extension accommodated by each of the NE and WNW-trending grabens, we distinguish two second-order stress provinces separated by a line running from the Naupaktos in the north to the Meligala in the south (Fig. 3: X–X′).

#### 4.1.1. Second-order province B1

The NE-trending set of grabens accommodated most of the extension and began to develop earlier. For instance, in the Pyrgos area, the Lapithas Fault (LF) and the Vounargos Fault (VF) (Fig. 3) caused the deposition of sediments ranging from Lower Pliocene to Holocene (Hageman, 1977; Koukouvelas et al., 1996). Further north, the Rio graben (Fig. 3, cross-section A–A′), with a length of about 30 km and a width of 10 km, shows maximum subsidence of the order of 1800 m (Doutsos et al., 1988). The second set of WNW-oriented grabens is associated with Pleistocene sediment accumulation and accommodates only a small amount of the regional extension, as is indicated by the slightly rotated beds and the small displacements (up to 500 m) occuring along these faults. These WNW-trending grabens are morphologically defined by major drainage courses (e.g. Alfios river), lakes (e.g. Trihonis lake) and shallow gulfs (e.g. Patras and Amvrakikos gulfs).

The state of stress in this province is complex. In cases where one set of grabens dominates, the $\delta_3$ axis trends NNE (Fig. 3, stereonet $SPB_5$) or NW (Fig. 3, stereonet $SPB_3$), corresponding to WNW (e.g. Nedas graben) or NE (e.g. Ambelon graben) trending grabens, respectively. However, in most cases, such as in the Pyrgos and Patras areas, both set of grabens are active and the $\delta_3$ axis trends almost N–S (Fig. 3, stereonets $SPB_1$, $SPB_4$). This $\delta_3$ axis trends parallel to the intersection between the master faults of the two sets of grabens, indicating the direction of tectonic transport in that area (*sensu* Scott et al., 1994).

#### 4.1.2. Second-order province B2

Most of the extension in this province is taken up by four WNW-trending asymmetric grabens: the Corinth, Tithorea, Atalanti and Almyros grabens (Fig. 3, $SPB_2$, $SPB_7$, $SPB_9$). The asymmetry of these grabens is mainly induced by N-dipping master faults, which are segmented along strike (Doutsos and Poulimenos, 1992). The age of the synrift deposits ranges from Early Pliocene in the east (e.g. Megara graben; Papp and Steininger, 1979) to Pleistocene in the west (Frydas, 1991; e.g. Sperhios graben, and western part of the Corinth graben), suggesting that the grabens propagated westwards (Doutsos et al., 1988). In the western part of the Corinth graben, seven N-dipping faults bound a series of crustal blocks, down to a depth of ~10 km (Fig. 3, cross-section B–B′). These faults show displacements up to 1000 m and are associated with wedge-shaped sedimentary prisms deposited during the Quaternary. The northern part of cross-section B–B′ shows an asymmetric graben 400 m below sea level bounded to the south by the Gulf of Corinth master fault, which forms a 300-m-high submarine escarpment (Brooks and Ferentinos, 1984). The Gulf contains about 1-km-thick Quaternary sediments (Brooks and Ferentinos, 1984) and the maximum structural relief

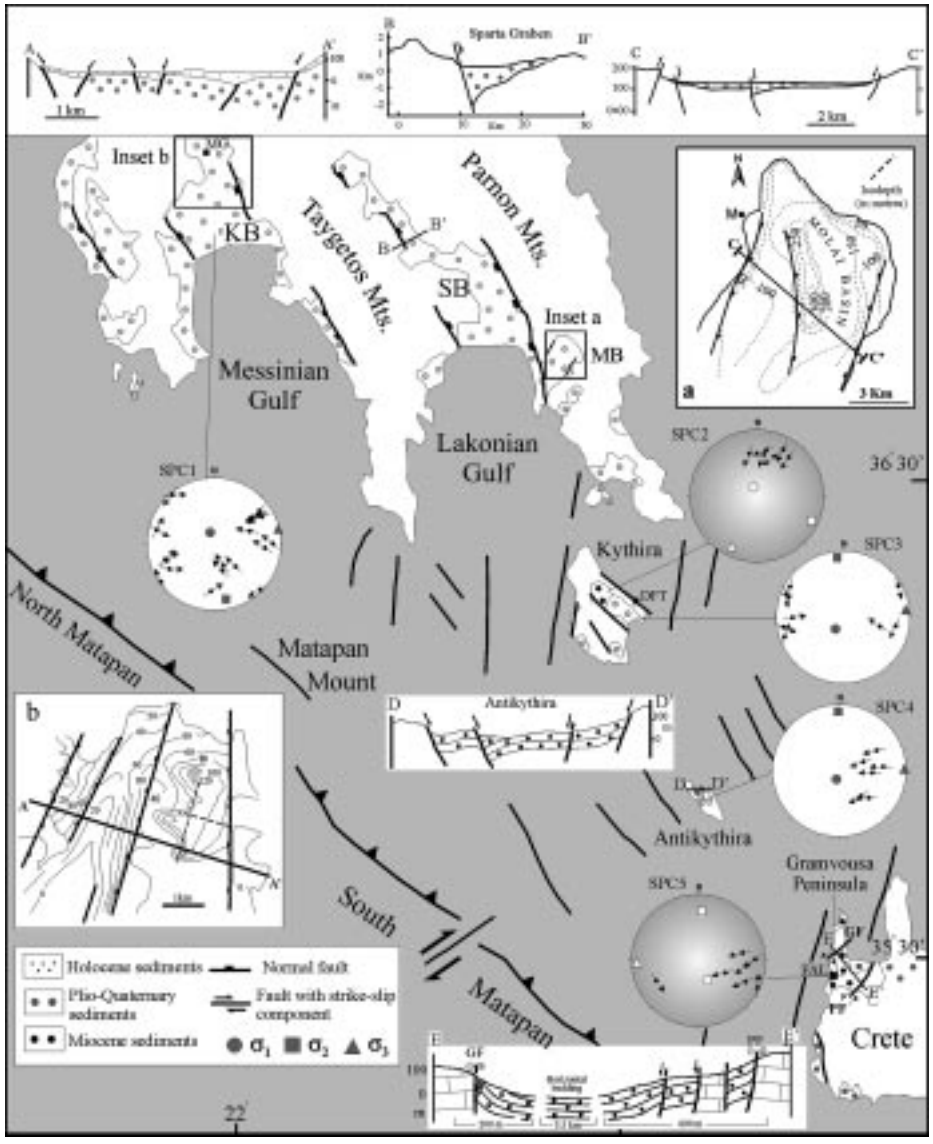


Fig. 4. Map of southwestern Aegean area (stress province C). Stereonets with white coloring are related to the Plio-Quaternary evolution. Stereonets with grading grey coloring show fault populations active throughout the L. Miocene-Plio-Quaternary time span. Inset a: Molai basin, M = Molai town. Cross-section C–C′ shows the subsurface geometry of Molai basin. Inset b: Structural lines, from the contact between Pliocene and Quaternary deposits, are derived from 40 borehole data in the Kalamata basin. A–A′: cross-section showing the subsurface geometry of the Pamisos Plain in Kalamata basin. KB = Kalamata basin, MB = Molai basin, SB = Sparta basin. GF = Gramvousa fault, PF = Platanos fault, FAL = Falasarna, DFT = Diakofti village.

between the lowest bedrock areas under the Gulf and the adjacent mountains is ~4 km. Further east, marine terraces in the footwall of the Gulf of Corinth master fault were uplifted to 600 m above sea level during the last 500 000 years, indicating uplift rates of the order of 1 mm/year (Keraudren and Sorel, 1987; Jackson and McKenzie, 1984).

Most of the earthquake epicenters are concentrated in the Gulf of Corinth, showing that the bulk of the tectonic activity takes place in this area. However, ocassional large ($Ms > 5.5$) earthquakes have occurred onshore, such as in the vicinity of the Kalavryta, Trikala and Klenia villages (Fig. 3). Indications of recent tectonic activity in this onshore domain come from strips of fresh limestone along the base of prominent fault scarps (Koukouvelas et al., 1999) and the occurrence of a large number of smaller faults which control sedimentation and define morphological steps in late Quaternary marine terraces (Dufaure et al., 1975; Doutsos and Piper, 1990). In contrast, Armijo et al. (1996) claimed that most of the extension in the Corinth graben takes place along a single fault, the coast-bounding Xylokastro Fault. Specifically, displacement rates of the order of 5–7 km and slip-rates of $10 \pm 3$ mm/year along this fault have been estimated based on three assumptions: (1) that the Xylokastro Fault is connected to a prominent offshore fault described by Brooks and Ferentinos (1984); (2) that the footwall of this fault was uplifted without internal deformation throughout the Quaternary; and (3) that regional uplift is not essential. However, these

assumptions are questionable. Firstly, there is not sufficient geophysical data to demonstrate that the Xylokastro Fault merges into the offshore fault, so this assumption is considered arbitrary (see Lyberis et al., 1998). Secondly, the footwall of Xylokastro Fault is strongly deformed by a series of active normal faults with a displacement often in excess of 500 m (figs. 3 and 4, in Poulimenos et al., 1989). Thirdly, east of the Xylokastro Fault, on another major normal fault, the Eliki Fault, Stewart and Vita-Finzi (1996) estimated that coseismic footwall uplift probably contributed only a minor proportion (~20%) of the observed coastal uplift over the last 3000 years (see also discussion in Jackson, 1999).

Only a small amount of the extension in the stress province *B2* is accommodated by NE-trending grabens, as in the case of the southeast part of the Corinth graben (Fig. 3, stereonets $SPB_6$, $SPB_8$; Roberts, 1996; Koukouvelas et al., 1999). Further north, NE-trending faults interact with WNW-trending faults producing large earthquakes, such as the 1981 ($M_L = 6.7$) event in the Alkyonides Gulf, and the 1954 ($M_L = 6.7$) earthquake in Sophades (see fig. 3 in Poulimenos and Doutsos, 1996).

### 4.2. Late Miocene evolution

During the Late Miocene most of this area had a high topographic relief (Schneider, 1972; Kowalczyk et al., 1977), and therefore information is lacking on stress and deformation during this time interval. In the Limni and Kymi basins (North and central Evia Island, Fig. 3) lacustrine and fluviatile sediments of Late Miocene age (Katsikatsos et al., 1981) are controlled by variably oriented normal and oblique normal faults (Fig. 3, stereonet $SPB_{10}$). Some of these faults are of synsedimentary origin. The computed stress field is similar to that derived from the Late Miocene deposits in the Mesohellenic Trough described above. Thus, we argue that during this period a consistently oriented stress system operated, with the $\delta_2$ axis oriented parallel to the mountain chain and with the $\delta_3$ axis oriented WSW–ENE, perpendicular to it (Fig. 3, stereonet $SPB_{11}$).

Furthermore, it seems very probable that this regime has affected the Thessalian basins, which lie between the Mesohellenic Trough and the Limni basin (Fig. 3). This is because continental deposits containing the *Pikermi* fauna of latest Miocene times (Melentis and Schneider, 1966) are aligned parallel to the NW trending faulted margins of the eastern Thessalian basin (Doutsos, 1980; Caputo and Pavlides 1993).

### 4.3. Summary

We consider that Plio-Quaternary extensional tectonics in the central Hellenic Peninsula are characterized by the interplay between ENE- and WNW-trending grabens. The WNW-trending grabens may have propagated westwards and are dominant in the eastern part of the area. The $\delta_3$ axis during the Late Miocene had a WSW–ENE orientation.

## 5. The southwestern Aegean area (stress province C)

This area extends from south Peloponnese through Kythira and Antikythira islands to the western edge of the Crete island (Fig. 4). Angelier et al. (1982) postulated a change of $\delta_3$ direction from WNW–ESE in the Pliocene–Lower Pleistocene to WSW–ENE in the Late Pleistocene. A similar change of $\delta_3$ orientation was also described by Mercier et al. (1989) with the difference that during the late Pleistocene, in the south Peloponesse, the stress system operated with a $\delta_3$ axis in a NW direction. Lyberis et al. (1982) mapped NNW- and NNE-trending normal faults that were active throughout the Plio-Quaternary and which are compatible with a NE–SW to E–W direction of $\delta_3$. Finally, Armijo and Lyon-Caen (1992) emphasized the role of east–west extension from the late Pliocene (~2–4 Ma) until the present day. Our results are in agreement with Lyberis et al. (1982), but we present evidence that the NNE-trending fault set, at the western edge of Crete, began to be active in the Late Miocene.

### 5.1. Plio-Quaternary evolution

In south Peloponnese, NW-trending grabens began to develop in the Early Pliocene, as is evident from fossiliferous marine deposits (Freyberg, 1967; Kowalczyk et al., 1977). These grabens remained active until the present, and divide the area into three peninsulas. Uplifted marine terraces along the coast of these peninsulas are cross-cut by NW-trending normal faults (Kelletat et al., 1976; Kowalczyk and Winter, 1979; Zelilidis and Doutsos, 1992). In the Sparta graben to the east, the Sparta Fault strikes parallel to the eastern front of the Taygetos Mountain (Fig. 4) and forms a steep escarpment (as much as 700 m in height), which was reactivated in historical times during a $M_L \sim 7$ earthquake event (Armijo and Lyon-Caen, 1992). Estimated footwall uplift and maximum downthrow movements along the Sparta Fault are ~1200 and ~2500 m, respectively (Fig. 4, cross-section B–B′; Doutsos et al., in press). Further west, fault-slip data derived from large-scale faults within the Kalamata graben are compatible with an ENE-directed $\delta_3$ (Fig. 4, stereonet $SPC_1$).

Another set of N- to NNE-striking normal and oblique normal faults form young scarps in the south Peloponnese and southeast Kythira. In the northern end of the Kalamata basin, small-scale fault scarps strike N–S (Fig. 4: inset b), dip westward at 70° and display normal-slip striations on slickensides. To the west, structural contours from the Pliocene/Pleistocene boundary, derived from data from 40 boreholes, reveal the presence of an 8-km-wide NNE-trending half-graben (Fig. 4: inset b, cross-section A–A′; Zelilidis and Doutsos, 1992). Similar structures controlled the trend of structural contours further to the southeast,

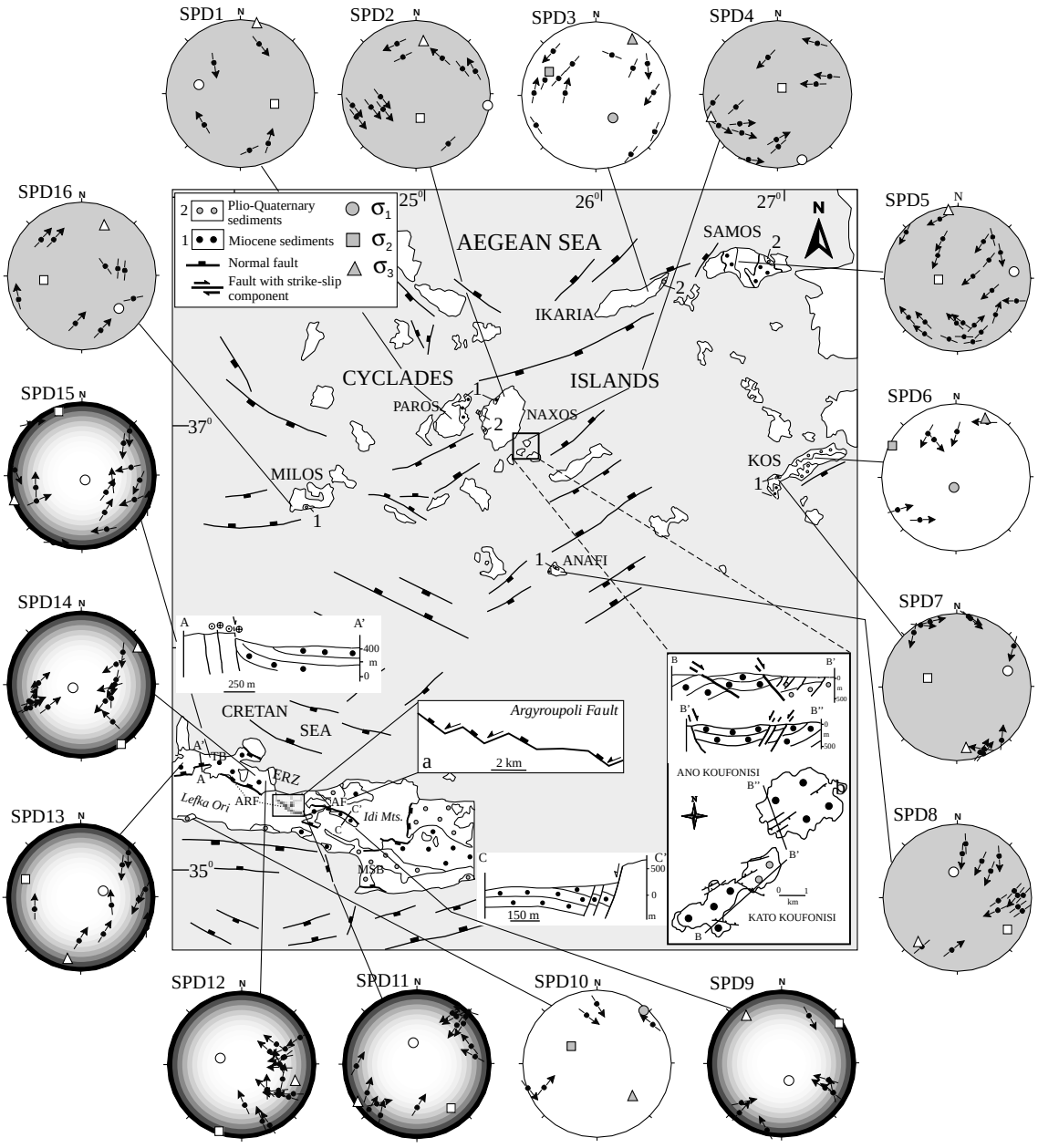


Fig. 5. Simplified map of the central part of the Hellenic Arc (stress province D). For stereonets with different shading see explanations in Figs. 2 and 4. AF = Amari Fault, ARF = Argyroupolis fault, ERZ = Episkopi rift zone, MSB = Messaras basin, TB = Topolia basin. Chronostratigraphic data for the Late Miocene: Paros (Dermitzakis and Papanikolaou, 1980), stereonet $SPD_1$; Naxos (Roesler, 1978), stereonet $SPD_2$; Koufonisia (Roesler, 1978), stereonet $SPD_4$; Samos (Theodoropoulos, 1979), stereonet $SPD_5$; Kos (Boger et al., 1974), stereonet $SPD_6$; Anafi (Reinecke et al. 1982), stereonet $SPD_8$; Milos (Fytikas, 1977), stereonet $SPD_{16}$-Chronostratigraphic data for the Plio-Pleistocene: Ikaria (Ktenas, 1969), stereonet $SPD_3$; Kos (Smith et al., 1995), stereonet $SPD_7$).

within the Molai graben (Fig. 4, inset a, cross-section C–C′). Recently, during the September 1986 ($M_L = 5.8$) Kalamata earthquake, a 6-km-long NNE-striking seismic fault was formed along the western front of the Taygetos Mountain. Displacements which occurred along the 50° dipping fault surface showed normal slip (Lyon-Caen et al., 1988).

In the southeast Kythira, near Diakofti, large fault scarps strike NNE–SSW, dip at 80° to the west–southwest, and display oblique-normal-slip striations (Fig. 4, stereonet $SPC_3$). Since bathymetric contours around the Kythira island trend NNE–SSW, it seems likely that the NNE-trending faults controlled the evolution of offshore basins in that area (Mascle et al., 1982). Further south along the western coast of Crete, De Chabalier et al. (1992) defined this transtensional regime using microseismic studies.

### 5.2. Late Miocene evolution

In Kythira Island, NW-trending grabens are filled with

early-Late Miocene to Pliocene marine deposits (Christodoulou, 1965; Meulenkamp et al., 1977). Synsedimentary faults within these grabens, as well as the tilting of Late Miocene strata prior to Pliocene deposition, suggest that the tectonic activity started in the Late Miocene (Lyberis et al., 1982). This tectonic activity has continued from the Late Miocene until present, as is evident from recent fault scarps at the graben margins. The computed $\delta_3$ axis responsible for the formation of these grabens is oriented NE (Fig. 4, stereonet $SPC_2$). Southwards to the Antikythira Island, NW-trending faults are sparse, whereas NNE-trending faults become important (Fig. 4, stereonet $SPC_3$, cross-section D–D′).

At the western edge of Crete Island, the Falasarna basin contains Late Miocene deposits (Meulenkamp et al., 1977; Frydas and Keupp, 1996) and is bounded by two left-lateral normal faults: the Gramvousa and the Platanos faults (Fig. 4). Deformation within the Falasarna basin is partitioned, as is the case of many basins associated with strike-slip duplexes. Here, steeply dipping fault zones and strongly rotated beds at the basin margins bound a wide undisturbed central area (Fig. 4, cross-section E–E′, stereonet $SPC_5$).

### 5.3. Summary

Since the Late Miocene, the locus of rifting, involving both NW- and NNE-trending extensional structures, migrated between western Crete and Peloponnese. The NNE-trending faults constitute a complex strike-slip zone between Kythira and Crete that has a long tectonic history from the Late Miocene to the present day.

## 6. The central part of the Hellenic Arc (stress province D)

This area comprises the eastern Cycladic islands, the Cretan Sea and the western–central part of Crete island (Fig. 5). Earlier studies by Angelier et al. (1982) and Mercier et al. (1989) inferred that a radial tensional regime had been active in Crete throughout the Plio-Pleistocene. For the Cycladic islands further north, these studies claimed that a change in the $\delta_3$ direction had occurred, from NE–SW in the Pliocene–Lower Pleistocene to NW–SE in the Middle Pleistocene to present day. Here, we present evidence that a non-orthogonal extension system, including WNW-trending normal and NE-trending transfer faults, has affected the central part of the Hellenic Arc from the Late Miocene until present day.

Western Crete is cross-cut by a 70-km-long WNW-trending rift: the Episkopi rift (Fig. 5). Two opposed-dipping faults, the Amari and Argyroupolis faults, form an antithetic relay structure in the central part of this rift zone. The Amari Fault, in the east dips to 75° to the southwest, has an arcuate shape in map view and forms a 300-m-high escarpment. Striations on the main slip plane of the Amari Fault, and on smaller nearby synthetic faults, indicate normal-slip movement (Fig. 5, stereonet $SPD_{11}$). A thick sequence (>400 m) of Neogene to Quaternary deposits (Meulenkamp et al., 1988) is faulted against the fault scarp and exhibits a strong (up to 40°) synthetic sense of rotation (Fig. 5, cross-section C–C′). In the west, the Argyroupolis Fault forms a 500-m-high escarpment and dips at 65° to the northeast. It is segmented along strike, comprising long WNW- and short ENE-trending fault segments (Fig. 5: inset a). Striations on the main slip plane of the Argyroupolis Fault show downthrow of the hanging wall toward the ENE, suggesting that the small ENE-trending, steeply dipping oblique-slip faults act as transfer faults. Footwall uplift along the Argyroupolis and Amari faults has contributed to the exhumation of HP/LT metamorphic rocks of the Lefka Ori and Idi Mountains, respectively.

The Episkopi rift zone is limited by two ENE-trending step-over zones: the Topolia basin in the north and the Messaras basin to the south (Fig. 5, TB and MB). In the Topolia basin, deformation is concentrated at the southern margin of the basin. Along this margin, a steeply dipping fault controlled the deposition of fan deltas and mudstone slumps (Kontopoulos et al., 1996), which are strongly rotated by smaller synthetic faults (Fig. 5, cross-section A–A′). Further north, the central part of the basin displays lesser tectonic activity, as is evident from horizontal bedding and sparse faulting. Striations on slip planes of the basin-bounding fault and on smaller faults are compatible with a tension direction ($\delta_3$) which varies between NNE–SSW and ENE–WSW (Fig. 5, stereonets $SPD_{13}$, $SPD_{15}$). These spatial variations represent local tension directions, which vary depending on the magnitude of the shear strain induced by the basin-bounding, strike-slip fault. Further east, the Messaras basin displays similar kinematic characteristics to the transtensional Topolia basin. It seems possible, therefore, that these faults transfer the extensional deformation from the Episkopi rift zone into the offshore extensional domains north and south of Crete.

This non-orthogonal extension system of WNW-trending normal faults and ENE-trending transfer faults seems to be typical of both the Cretan Sea and the eastern Cycladic islands (Fig. 5). Thus, WNW- and ENE-trending faults appear to have controlled the evolution of the post-Late Miocene sedimentary basins (Roesler, 1978) in the Koufonisia islands (Boronkay and Doutsos, 1994; Fig. 5: inset b, cross-sections B–B′ and B′–B″). Similar to the Topolia basin in Crete and to the Cycladic islands, the trend of $\delta_3$ axes varies between NNE–SSW and ENE–WSW with an average trend of NE–SW (Fig. 5). As appears to be the case in Crete, the strong variation in the orientation of $\delta_3$ seems to be the result of simple shearing generated along the transfer zones.

### 6.1. Summary

We infer that since the Late Miocene, extension in the central part of the Hellenic Arc has taken place in the style

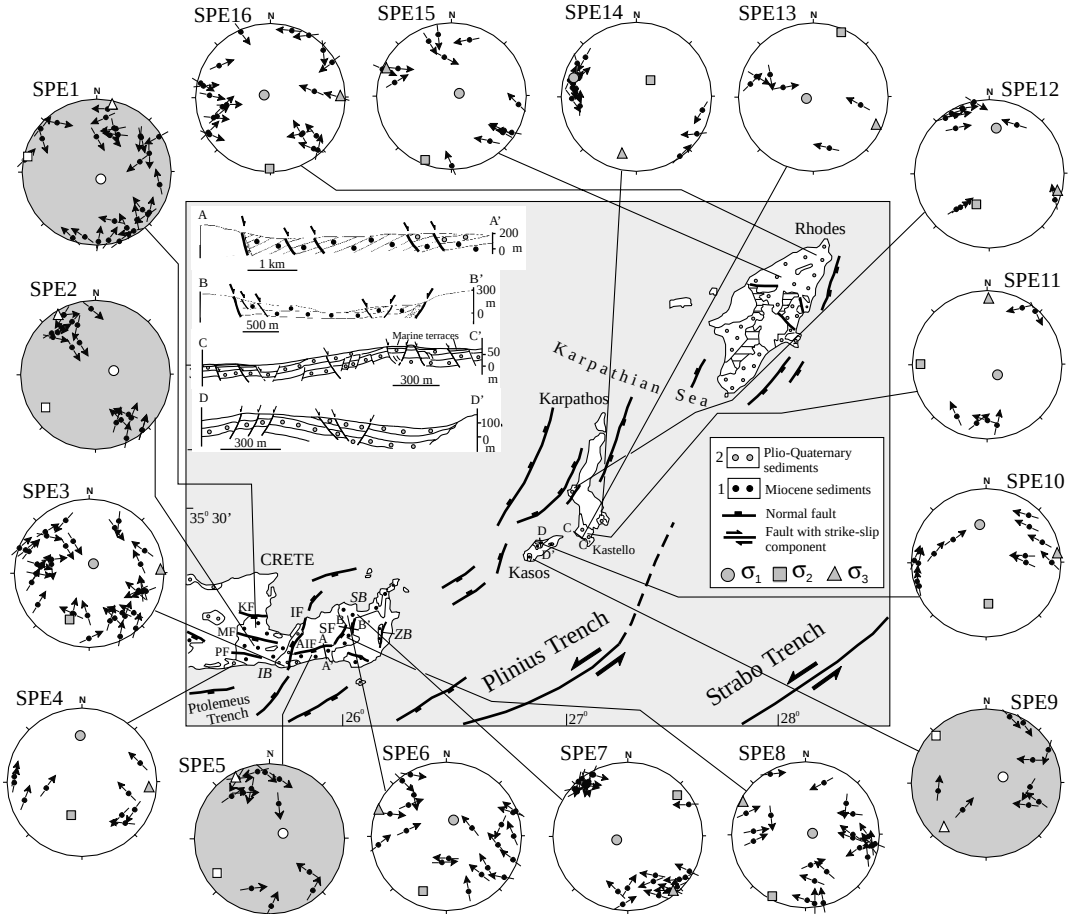


Fig. 6. Simplified map of the south-eastern Aegean area (stress province E). For stereonets with different shading see Figs. 2 and 4. IB = Ierapetra basin, SB = Sitia basin, ZB = Zakros basin, AIF = Agios Ioannis Fault, KF = Kritsa Fault, IF = Ierapetra Fault, SF = Sitia Fault, MF = Makrilia Fault, PF = Parathiri Fault.

of oceanic ridge-transform systems. The average trend of $\delta_3$ is NE (35°E) and the local deviations of $\delta_3$ orientations are probably caused by variations in the shear magnitude acting along the transfer fault zones.

## 7. The southeastern part of the Hellenic Arc (stress province E)

This area comprises the eastern part of Crete, Kasos, Karpathos and Rhodes islands (Fig. 6). A roughly NW–SE orientation of $\delta_3$ throughout the Plio-Pleistocene is postulated by Angelier et al. (1982) and Mercier et al. (1989). In contrast, Armijo and Lyon-Caen (1992) emphasize the role of E–W tension at the eastern end of the Hellenic Arc. Below, we recognize an earlier phase of NNE- to NNW-directed tension during the Late Miocene, followed by a younger phase of E–W trending tension in the Plio-Pleistocene.

### 7.1. Plio-Pleistocene evolution

In the western Karpathos Island, Late Pliocene sediments (Buttner and Kowalczyk, 1978) are faulted against an ENE-trending left-lateral strike-slip fault (Fig. 6), which strikes parallel to a large offshore fault mapped by Martin and Mascle (1989). Fault-slip data collected from smaller strike-slip faults within this basin are compatible with an E–W orientation of $\delta_3$ (Fig. 6, stereonet $SPE_{12}$). Further south in the Kastello Peninsula, Tyrrhenian marine terraces (Barrier et al., 1979; Keraudren and Sorel, 1984) are cross-cut by oblique-normal faults, which are consistent with an E–W orientation of $\delta_3$ (Fig. 6, stereonet $SPE_{13}$, cross-section C–C′). In addition, fault-slip data collected from oblique-normal faults within Late Pliocene sediments from Rhodes Island (Mutti et al., 1970) are consistent with a tension direction similar to that on Karpathos Island (Fig. 6, stereonets $SPE_{15}$, $SPE_{16}$). In Kasos Island, Pliocene sediments (Barrier and Angelier, 1982) are cut by a fault population consisting of N-trending strike-slip faults and NW-trending oblique-normal faults, indicating a stress regime with $\delta_3$ orientated in an E–W direction (Fig. 6, stereonet $SPE_{10}$, cross-section D–D′).

In the eastern Crete, Pliocene deposits (Fortuin, 1978) are cross-cut by oblique-normal faults, which trend mainly

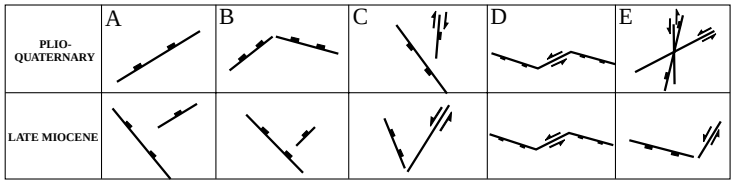
PLIO-QUATERNARY
LATE MIOCENE
A
B
C
D
E

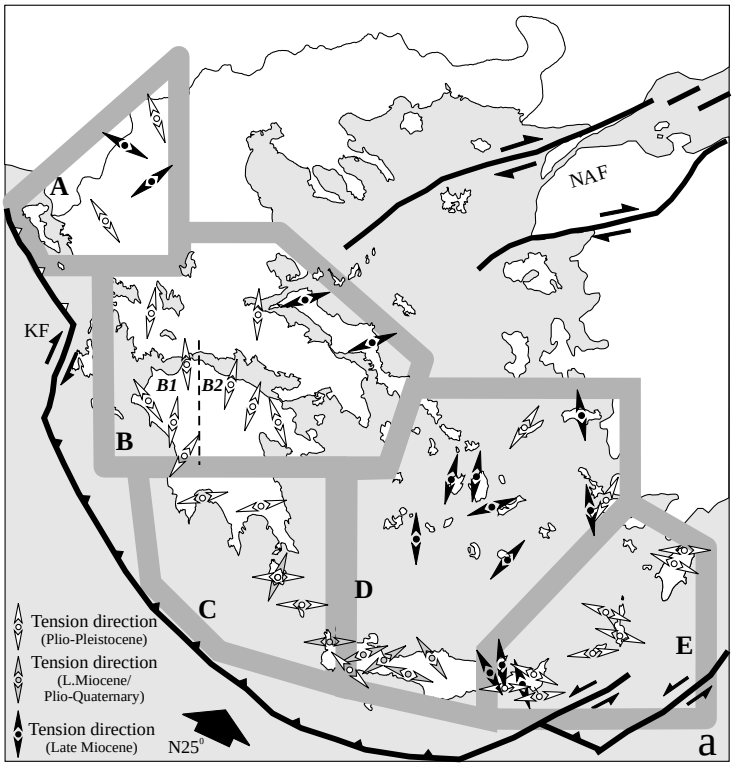
A
B
C
D
E
B1
B2
KF
NAF
Tension direction
(Plio-Pleistocene)
Tension direction
(L.Miocene/
Plio-Quaternary)
Tension direction
(Late Miocene)
N25°
a

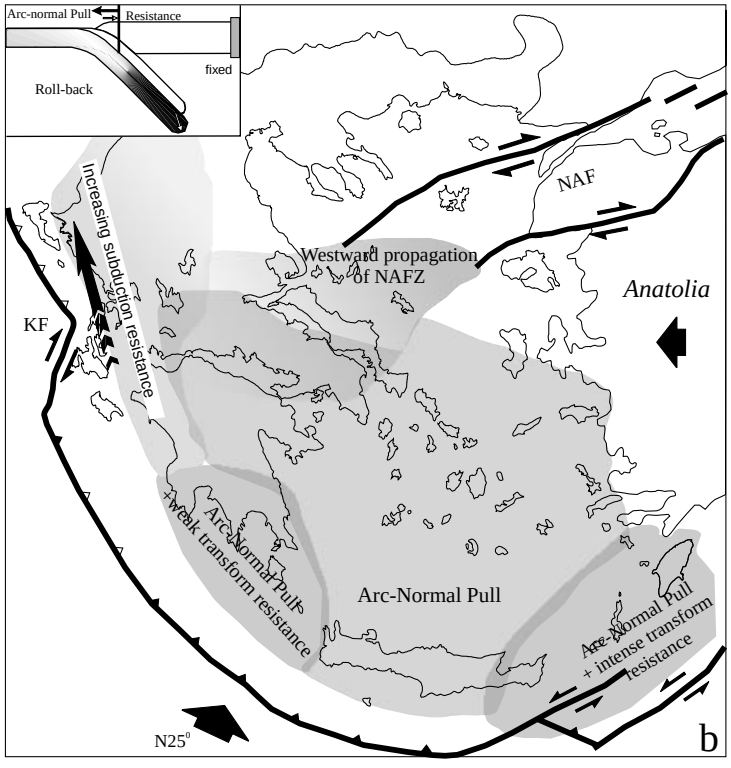
Arc-normal Pull
Resistance
fixed
Roll-back
Increasing subduction resistance
NAF
Westward propagation
of NAFZ
Anatolia
KF
+weak transform resistance
Arc-Normal Pull
Arc-Normal Pull
Arc-Normal Pull
+ intense transform
resistance
N25°
b

NE–SW (Fig. 6, stereonets $SPE_3$, $SPE_4$). Most of the extension is taken up by the Ierapetra Fault, which is a major structural element cutting across eastern Crete and continuing offshore. Recent deformation along this fault is documented by an impressive 600-m-high fault scarp and its associated young colluvial and alluvial apron. Further to the east, two NE-trending faults controlled the subsidence of two asymmetric basins, the Sitia basin to the west (Fig. 6, section B–B′) and the Zakros basin to the east. Although some stereonets (Fig. 6, stereonets $SPE_6$, $SPE_7$, $SPE_8$) are derived from fault populations collected within Late Miocene sediments, the fact that in places these faults cut the whole rock sequence from Late Miocene to Plio-Quaternary leads us to assume that these areas have been affected intensively by the Plio-Quaternary tectonism.

The fault population consists of numerous ENE-trending left-lateral faults (Fig. 6, $SPE_{12}$, $SPE_3$, $SPE_7$), and second-order N-trending left-lateral faults (Fig. 6, stereonets $SPE_{14}$, $SPE_4$) and NE-trending oblique-normal faults (Fig. 6, stereonets $SPE_{13}$, $SPE_3$, $SPE_6$, $SPE_{15}$, $SPE_{16}$). This fits well with a theoretical incremental strain pattern of associated strike-slip faults (P- and R-shears) and pull-apart extension of structures predicted by left-lateral simple-shear along large-scale ENE-trending faults.

### 7.2. Late Miocene evolution

In the eastern Crete, three WNW-trending faults—the Kritsa, Makrilia and Parathiri faults—are often associated with limestone breccia slumps and slides, suggesting a synsedimentary origin (Fortuin 1978; Ten Veen and Postma 1999). Striations on slip planes of these basin-forming faults indicate left-lateral, oblique-normal movements. Smaller NE-trending, oblique-normal to strike-slip faults act as transfer faults, and with the WNW-trending faults constitute a non-orthogonal extensional system. The computed tension direction ($\delta_3$) changes from NNE to NNW (Fig. 6, stereonets $SPE_1$, $SPE_2$).

The Ierapetra Fault trends parallel to the aforementioned transfer zones and separates Late Miocene sediments from basement rocks. We consider it likely that this fault has also been active since the Late Miocene. East of this fault zone, structural lineaments within the basement change direction, from a WNW trend in the west to a ENE trend in the east (Kokkalas and Doutsos, in press). The Agios Ioannis Fault (AIF) trends parallel to these structural lines and exhibits a synsedimentary origin, as is evident from observed rapid changes in sedimentary facies and the wedge-shaped sedimentary prisms in its hanging wall. Oblique-normal faults and strike-slip faults within this sedimentary prism (Fig. 6, cross-section A–A′, stereonet $SPE_5$) suggest that simple-shearing on ENE-trending faults, which characterize the younger extensional phase, is likely to have commenced earlier in this area, probably during the Late Miocene.

Late Miocene sediments in the easternmost part of the Hellenic Arc are found only as small erosional remnants in Karpathos Island. Therefore we assume that the area was above sea level at that time, as was the Peloponnese in the western part of the Arc.

### 7.3. Summary

During the Plio-Pleistocene, the southern part of the Hellenic Arc was strongly affected by simple shearing acting along left-lateral ENE-trending faults. P- and R-shears and pull-apart structures have been recorded, and a local E–W tension direction ($\delta_3$) appears to have characterized the stress field. This phase seems to have begun earlier in the easternmost Crete, during the Late Miocene. West of the Ierapetra Fault, extension during the Late Miocene was accomplished by WNW- and NE-trending faults. The inferred stress field shows a change in the $\delta_3$ orientation from NNE–SSW to NNW–SSE.

## 8. Geodynamic interpretation of the Aegean stress map

In the following section, we try to relate spatial and temporal variations of the intraplate stress field in the Aegean area to the plate-tectonic forces acting along the Hellenic Arc–Trench system. For this purpose, we adopt the terminology of Meijer and Wortel (1997) for the forces acting on the Aegean lithosphere boundary (Fig. 7b: inset). Arc-normal pull exerted on the overriding plate is caused by roll-back of the subduction zone and by the potential energy difference between the Aegean lithosphere and the Mediterranean lithosphere. Subduction resistance results from shearing between the overriding plate and the subduction zone.

### 8.1. Stress province A

At present time, this area undergoes extension, whereas compression is situated further to the west, along the Ionian islands and the western Hepirus (Mercier et al., 1972; Doutsos et al., 1987; Hatzfeld et al., 1995), where the Adriatic plate collides with northern Greece (Fig. 7; Anderson and Jackson, 1987). This collisional zone is separated from the Hellenic Arc to the south by a large dextral strike-slip fault, the Kefallonia Fault (Fig. 7; Papazachos and Kiratzi, 1996; Cocard et al., 1999).

Fig. 7. (a) Stress and fault pattern in the Aegean area deduced from structural analysis of faults from Late Miocene to the Plio-Quaternary. Double arrowheads with filled circles show the tension direction computed from striations measured on fault planes. The dashed line roughly separates the sub-provinces B1 and B2. Rectangles define the different stress provinces discussed in the text. Grey-colored border lines indicate the existence of transitional zones between the stress provinces. (b) Schematic illustration of the forces acting on the boundary of the Aegean lithosphere. Inset shows the main forces acting on a converging plate boundary (after Meijer and Wortel, 1997). The right edge of the overriding plate is fixed, representing the non-deforming Eurasian plate.

Strong coupling and resistance of the colliding plates may allow the transmission of the horizontal compressive forces from the subducting Adriatic plate to the overriding Aegean plate. As a result, NE-trending grabens (with $\delta_3$ in a NW direction) were formed parallel to the direction of plate convergence, determined by seismic studies (Papazachos and Kiratzi, 1996).

During the Late Miocene, a NE trending $\delta_3$ axis caused the formation of NW-trending grabens which are oriented parallel to the isopic zones of the Hellenides. They can be interpreted as the result of collapse of an overthickened crust established during the main middle Miocene phase of the Alpine orogeny (Doutsos, 1980; Caputo and Pavlides, 1993).

### 8.2. Stress province B

This stress province lies between the southern prolongation of the North Anatolian Fault (NAF) to the east and a compressional belt of the Ionian islands in the west, which is associated with the subduction of oceanic to intermediate crust of the Ionian abyssal plain and the Mediterranean Ridge beneath the western Peloponnese (Leydecker et al., 1978; Makris and Stobbe, 1984; Underhill, 1989). The subduction zone shows a gently dipping segment below the western Peloponnese and a steeply dipping segment further to the east (fig. 3 in Papazachos et al., 2000). The Nafpaktos–Meligala line (Fig. 3), where this change in the dip of the subduction occurs, separates the B1 stress province in the west from the B2 stress province in the east. As in the case of stress province A, NE-trending rifts on the overriding Aegean plate probably indicate resistance to subduction. From stress provinces B2 to B1, the coupling of the converging plates appears to increase and consequently the NE-trending rifts become more important.

Since the Late Pliocene, the WNW-trending rifts seem to have propagated gradually westward from stress province B2 to stress province B1, i.e. from the Aegean Sea to the Ionian Sea. The latter structures are considered to be the result of a pull-apart mechanism in the accommodation zone between the Kefallonia zone and the NAF (Reuther et al., 1993; Kahle et al., 1998). Although slip rates estimated for the Kefallonia Fault are large (~2.7 cm/year, Louvari et al., 1999), it is doubtful that slip rates at the southern prolongation of the NAF, in the Sporades Trough, are large enough to produce extensive rifting in the Hellenic Peninsula. It is more likely that these rifts represent pull-apart structures within an area that lies between stable Europe and the southwestward moving South Aegean area. However, it is important to note that only a part of this motion may be due to the motion of the Anatolian plate; the remaining motion reflects arc-normal pull of the Aegean plate margin in stress province C (see below).

Similar to stress province A, the $\delta_3$ axis trends in a NE direction during the Late Miocene and is associated with collapse structures that formed after the culmination of the main orogeny. Thus, the NAF seems to have affected the Hellenic Peninsula in post-Late Miocene time.

### 8.3. Stress province C

This stress province is located behind the Matapan Trench (Fig. 4). The northern end of this trench marks an important change in the convergence mechanism, from oceanic and quasi-continent/continent convergence in the north to oceanic/continent convergence to the south (Lyberis and Lallemant, 1985; Le Pichon and Angelier, 1979). NW-trending grabens aligned parallel to the Matapan Trench can be interpreted as the result of arc-normal pull acting on the Aegean plate margin.

Furthermore, N- to NNE-trending normal and oblique-normal faults in the area have been considered to be the result of incipient collision of the arc with the buoyant crust of the African margin (Lyon-Caen et al., 1988). However, all these structures strike in a more northerly direction than the average convergence direction ($025^0$E) in the area (Taymaz et al., 1991). More plausible may be the strain partitioning hypothesis from Le Pichon et al. (1995), who interpreted these structures as pull-aparts generated in the course of oblique subduction in the area. Right-lateral movements along the Matapan Trench may be responsible for the formation of these grabens, since the trench trends oblique to the convergence direction (Fig. 4). Strain partitioning here may be due to combination of arc-normal pull forces acting on the Aegean plate boundary and transform resistive forces acting along the subduction zone. In stress province C, the shallow-dipping segment of the subduction zone is shorter and steeper than in stress province B1 (compare Figs. 3 and 4 in Papazachos et al., 2000). Consequently, resistive forces may be weaker in stress province C than those acting in stress province B1.

Angelier et al. (1982) and Lyberis et al. (1982) describe a complex fault zone in the Kythira–Antikythira strait associated with the opening of the Cretan Sea. Along this fault zone, the Peloponnese block has rotated clockwise at 5°/Ma since the Early Pliocene (Laj et al., 1982). It is possible that this fracture zone also comprises the left-lateral strike-slip faults which since the Late Miocene have formed the Falasarna basin at the western edge of Crete. In this case, the Peloponnese block might have started to rotate earlier, perhaps during the Late Miocene.

### 8.4. Stress province D

This stress province lies opposite the Mediterranean Ridge accretionary complex. The accumulation of Late Miocene to Holocene sediments, up to 1000 m thick, in the central part of the Cretan Sea (Hsu et al., 1975), as well as the existence of up to 2400 m deep depressions (Mascle and Martin 1990), indicate that the area has been strongly extended (Angelier, 1979). Extension in the area is accommodated by WNW-trending normal faults that strike parallel to the Hellenic Trench and which have been active

since the Late Miocene. Simple shearing along NE- to ENE-trending transfer zones caused local variations in the tension direction between NNE–SSW and WSW–ENE.

A fault system with a similar geometry and kinematics appears to have affected the southwestern part of the Anatolian block (Hancock and Barka, 1987; Price and Scott, 1994; Westaway, 1993). In this area, NE-trending grabens, such as the Burdur, Baklan and Agicol grabens, formed as a result of differential stretching in the hanging wall of the WNW-striking Gediz graben (Sengor, 1987). It seems probable, therefore, that since the Late Miocene, NE-trending faults have transfered some of the motion of the Anatolian block toward the southern Aegean area. Westaway (1994) similarly considered the present-day slip rates observed in southwestern Anatolian (40 mm/year) to be the sum of slip rates along the North Anatolian Fault (20 mm/year) and local extension (20 mm/year).

We conclude that the appropriate mechanisms for stress province D involve arc-normal pull acting on the Aegean plate and the transfer of the motion of Anatolia along NE- to ENE-striking faults. We do not recognize significant extension along the arc in Crete, so we do not support the model of Le Pichon et al. (1995) concerning incipient collision between the Hellenic Arc and the African lithosphere (for discussion see also Duermeijer et al., 2000).

### *8.5. Stress province E*

This stress province extends behind the eastern termination of the Hellenic Trench. Southeast of Crete, the trench bifurcates into three ENE-striking branches: the Ptolemeus, Pliny, and Strabo trenches (Fig. 6). The angular deviation of 40° between the relative convergence direction of 025°E (Taymaz et al., 1991) and the trench orientation, as well as the remarkable rectilinearity of the trench itself, implies left-lateral motion along this structure (Le Pichon and Angelier, 1979).

Since the Late Miocene, a two-stage transtensional stress regime has been established in this area. The first stage, which comprises a NNE- to NNW-tension direction, can be associated with arc-normal pull of the Aegean plate boundary. The second stage, comprising ENE- and N-trending strike-slip faults as well as NNE-trending oblique-normal faults, represents the result of strain partitioning during oblique convergence at the eastern segment of the arc. They may have formed as a response to arc-normal pull and transform resistive forces.

## 9. Conclusions

The recognition of five stress provinces in the Aegean lead us to the following geodynamic aspects:

The central Aegean domain has been undergoing extension accommodated by WNW- and NE-trending faults since the Late Miocene. The area expands to the southwest as a result of two components of motion: (1) the motion of the Anatolian plate and (2) the arc-normal pull acting on the Aegean plate margin.

Transmission of horizontal compressive forces between the subducting Adriatic plate and NW-Greece caused the formation of NE-trending rifts in the Greek mainland and North Peloponnese.

Widespread strike-slip and normal faulting in the eastern segment and moderate oblique extension in the western segment of the arc formed by the combination of arc-normal pull acting on the Aegean plate and transform resistance acting on the subduction zone.

During the Late Miocene, the NW-directed rifting in the Hellenic Peninsula is associated with collapse of an overthickened crust, which was established in the Middle Miocene, during the late stages of the main orogeny.

Since the Early Pliocene, the WNW-trending rifts propagated westwards from the Aegean to the Ionian Sea and were likely generated as pull-apart structures formed between stable Europe and the rapidly extended southern Aegean area.

## Acknowledgements

The authors are grateful to Iain Stewart, Paul Meijer and an anonymous referee for their suggestions which greatly improved an earlier version of the manuscript.

## References

Anderson, H., Jackson, J., 1987. The deep seismicity of the Tyrrhenian Sea. Geophysical Journal of the Royal Astronomical Society 91, 613–637.

Angelier, J., 1979. Neotectonique de l'arc egeen, Societe Geologique du Nord

Angelier, J., 1994. Fault slip analysis and paleostress reconstruction. In: Hancock, P.L. (Ed.), Continental Deformation. Pergamon Press, Oxford, pp. 53–100.

Angelier, J., Goguel, J., 1979. Sur une methode simple de determination des axes principaux des contraintes pour une population de failles. Comptes Rendus de l'Academie des Sciences 288, 307–310.

Angelier, J., Mechler, P., 1977. Sur une methode graphique de recherche des contraintes principales egalement utilisable en tectonique et en seismologie: la methode des diedres droits. Bulletin de la Societe Geologique de France 7, 1309–1318.

Angelier, J., Lyberis, N., Le Pichon, X., Barrier, E., Huchon, P., 1982. The tectonic development of the Hellenic arc and the Sea of Crete: a synthesis. Tectonophysics 86, 159–196.

Armijo, R., Lyon-Caen, H., 1992. East–west extension and Holocene normal-fault scarps in the Hellenic arc. Geology 20, 491–494.

Armijo, R., Meyer, B., King, G.C.P., Rigo, A., Papanastasiou, D., 1996. Quaternary evolution of the Corinth Rift and its implications for the Late Cenozoic evolution of the Aegean. Geophysical Journal International 126, 11–53.

Barrier, E., Angelier, J., 1982. Structure et neotectonique de l'arc hellenique oriental: les iles de Kassos et Karpathos (Dodecanese, Greece). Revue de Geologie Dynamique et de Geographie Physique 23, 257–276.

Barrier, E., Muller, C., Angelier, J., 1979. Sur l'importance du Quaternaire ancien marin dans l'ile de Karpathos (Arc Egeen, Greece) et ses implications tectoniques. Comptes Rendus Sommaire Societe Geologique de France 5, 198–201.

Billiris, H., et al., 1991. Geodetic determination of tectonic deformation in Central Greece from 1900 to 1988. Nature 350, 124–129.

Boger, H., Gersonde, R., Willmann, R., 1974. Das Neogen im Osten der Insel Kos (Agais, Dodekanes)-Stratigraphie und Tektonik. Neus Jahrbuch fur Geologie und Palaontologie Abhalungen 145, 129–152.

Boronkay, K., Doutsos, T., 1994. Transpression and transtension within different structural levels in the central Aegean region. Journal of Structural Geology 16, 1555–1573.

Brooks, M., Ferentinos, G., 1984. Tectonics and sedimentation in the Gulf of Corinth and the Zakynthos and Kefallinia channels, western Greece. Tectonophysics 101, 25–54.

Brunn, J.H., 1956. Contribution a l'etude geologique du Pinde septentrional et une partie de la Macedoine occidentale. Annales Geologiques des Pays Helleniques 7, 358.

Buttner, D., Kowalczyk, G., 1978. Late Cenozoic Stratigraphy and Paleogeography of Greece—a review. In: Closs, H., Roeder, D., Schmidt, K. (Eds.), Alps, Appenines, Hellenides. Verlagbuchandlung, Stuttgart, pp. 494–501.

Caputo, R., Pavlides, S., 1993. Late Cenozoic geodynamic evolution of Thessaly and surroundings (central–northern Greece). Tectonophysics 233, 339–362.

Christodoulou, G., 1965. Quelques observations sur la geologie de Cythere et examen micropaleontologique des formations neogenes de l'ile. Bulletin of the Geological Society of Greece 6, 385–399.

Cocard, M., Kahle, H.-G., Peter, Y., Geiger, A., Veis, G., Felekis, S., Paradissis, D., Billiris, H., 1999. New constrains on the rapid crustal motion of the Aegean region: recent results inferred from GPS measurements (1993-1998) across the West Hellenic Arc, Greece. Earth and Planetary Science Letters 172, 39–47.

Davies, R.R., England, P.C., Parsons, B.E., Billiris, H., Paradissis, D., Veis, G., 1997. Geodetic strain of Greece in the interval 1892–1992. Journal of Geophysical Research 102, 24571–24588.

De Chabalier, J.B., Lyon-Caen, H., Zollo, A., Deschamps, A., Bernard, P., Hatzfeld, D., 1992. A detailed analysis of microearthquakes in western Crete from digital three-component seismograms. Geophysical Journal International 110, 347–360.

Dermitzakis, M., Papanikolaou, D., 1980. The molasse of Paros Island, Aegean Sea. Ann. Naturhist. Mus. Wien 83, 59–71.

Dewey, J., Celal Sengor, A.M., 1979. Aegean and surrounding regions: Complex multiplate and continuum tectonics in a convergent zone. Geological Society of America Bulletin 90, 84–92.

Doutsos, T., 1980. Postalpine geodynamic Thessaliens (Griechenland). Zeitschrift der Deutschen Geologischen Gesellschaft 131, 685–698.

Doutsos, T., Koukouvelas, I., 1998. Fractal analysis of normal faults in Northwestern Aegean area, Greece. Journal of Geodynamics 26, 197–216.

Doutsos, T., Piper, D.J.W., 1990. Listric faulting, sedimentation, and morphological evolution of the Quaternary eastern Corinth rift, Greece: first stages of continental rifting. Geological Society of America Bulletin 102, 812–829.

Doutsos, T., Poulimenos, G., 1992. Geometry and kinematics of active faults and their seismotectonic significance in the western Corinth–Patras rift (Greece). Journal of Structural Geology 14, 689–699.

Doutsos, T., Kontopoulos, N., Frydas, D., 1987. Neotectonic evolution of northwestern-continental Greece. Geologische Rundschau 76, 433–450.

Doutsos, T., Kontopoulos, N., Poulimenos, G., 1988. The Corinth-Patras rift as the initial stage of continental fragmentation behind an active island arc (Greece). Basin Research 1, 177–190.

Doutsos, T., Koukouvelas, I., Zelilidas, A., Kontopoulos, N., 1994. Intracontinental wedging and post-orogenic collapse in the Mesohellenic Trough. Geologische Rundschau 83, 257–275.

Doutsos, T., Koukouvelas, I., Poulimenos, G., Kokkalas, S., Xypolias, P., Skourlis, K. An exhumation model of the south Peloponnesus, Greece. Geologische Rundschau (in press).

Doutsos, T., Piper, G., Boronkay, K., Koukouvelas, I., 1993. Kinematics of the Central Hellenides. Tectonics 12, 936–953.

Drooger, C.W., Meulenkamp, J.E., 1973. Stratigraphic contributions to the geodynamics in the Mediterranean area: Crete as a case history. Bulletin of the Geological Society of Greece 10, 193–200.

Duermeijer, C.E., Nyst, M., Meijer, P.Th., Langereis, C.G., Spakman, W., 2000. Neogene evolution of the Aegean arc: paleomagnetic and geodetic evidence for a rapid and young rotation phase. Earth and Planetary Science Letters 176, 509–525.

Dufaure, J.J., Keraudren, B., Sebrier, M., 1975. Les terrasses de Corinthie: chronologie et deformations. Comptes Rendus de l'Academie des Sciences de Paris 281, 1943–1945.

Etchecopar, V., Vasseur, G., Daignieres, M., 1981. An inverse problem in microtectonics for the determination of stress tensors from fault striation analysis. Journal of Structural Geology 3, 51–65.

Fortuin, A.R., 1978. Late Cenozoic history of eastern Crete and implications for the geology and geodynamics of the southern Aegean area. Geologie en Mijnbouw 57, 451–464.

Freyberg, B., 1967. Die Neogen Diskordanz in Central Kythira. Praktika Akademias Athinon 42, 361–381.

Frydas, D., 1991. Palaookologische und stratigraphische Untersuchungen der Diatomeen des Pleistozans der N-Peloponnes, Griechenland. Bulletin of Geological Society of Greece 25, 499–513.

Frydas, D., Keupp, H., 1996. Biostratigraphical results in Late Neogene deposits of NW Crete, Greece, based on calcareous nannofossils. Berliner Geowissenschaftliche Abhandlungen 18, 169–189.

Fytikas, M., 1977. Geological map of Greece 1:20000, Milos Island. Institute of Geological and Mineral Exploration, Athens.

Gregor, H.J., Velitzelos, E., 1995. Facies development of Greek browncoals-dependent on tectonic movements. Annales Geologiques des Pays Helleniques 36, 731–739.

Hageman, J., 1977. Stratigraphy and sedimentary history of the Upper Cenozoic of the Pyrgos area (Western Peloponnesus, Greece). Annales Geologiques des Pays Helleniques 28, 299–333.

Hancock, P.L., 1985. Brittle microtectonics: principles and practice. Journal of Structural Geology 7, 437–457.

Hancock, P.L., Barka, A.A., 1987. Kinematic indicators on active normal faults in western Turkey. Journal of Structural Geology 9, 573–584.

Hatzfeld, D., Kassaras, I., Panagiotopoulos, D., Amorese, D., Makropoulos, K., Karakaisis, G., Coutant, O., 1995. Microseismicity and strain pattern in northwestern Greece. Tectonics 14, 773–785.

Hatzfeld, D., Martinod, J., Bastet, G., Gautier, P., 1997. An analog experiment for the Aegean to describe the contribution of gravitational potential energy. Journal of Geophysical Research 102, 649–659.

Hoeppener, R., 1955. Tektonik im Schiefergebirge. Geologische Rundschau 44, 26–58.

Hsu, K.J., Montadert, L., Bernouilli, D., Bizon, G., Cita, M., Erickson, A., Fabricius, F., Garrison, R.E., Kidd, R.B., Melieres, F., Muller, C., Wright, R.C., 1975. Site 378: Cretan Basin. In: Hsu, K.J., Montadert, L., et al. (Eds.), Initial Reports of the Deep Sea Drilling Project XLII. Scripps Institution of Oceanography, pp. 321–339.

Jackson, J.A., 1994. Active tectonics of the Aegean region. Annual Review Earth and Planetary Science 22, 239–271.

Jackson, J.A., 1999. Fault death: a perspective from actively deforming regions. Journal of Structural Geology 21, 1003–1010.

Jackson, J.A., McKenzie, D., 1984. Active tectonics of the Alpine-Himalayan Belt between western Turkey and Pakistan. Geophysical Journal of the Royal Astronomical Society 77, 185–264.

Jackson, J.A., Haines, J., Holt, W., 1992. The horizontal velocity field in the deforming Aegean Sea region determined from the moment tensors of earthquakes. Journal of Geophysical Research 97, 17657–17684.

Jackson, J.A., King, G., Vita-Finzi, C., 1982. The neotectonics of Aegean: an alternative view. Earth and Planetary Science Letters 61, 303–318.

Jacobshagen, V., 1986. Geologie von Griechenland. Berlin Gebruder Borntraeger, pp 363.

Kahle, H.-G., Straub, C., Reilinger, R., McClusky, S., King, R., Hurst, K., Kastens, K., Cross, P., 1998. The strain rate field in the eastern Mediterranean region, estimated by repeated GPS measurements. Tectonophysics 294, 237–252.

Katsikatsos, G., De Bruijn, H., Van der Meulen, A.J., 1981. The Neogene of the Island of Euboea (Evia), a review. Geologie en Mijnbouw 60, 509–516.

Kelletat, D., Kowalczyk, G., Schroder, B., Winter, K.P., 1976. A synoptic view on the neotectonic development of the Peloponnesian coastal regions. Zeitschrift der Deutschen Geologischen Gesellschaft 127, 447–465.

Keraudren, B., Sorel, D., 1984. Relations entre sedimentation, tectonique et morphologie dans le Plio-Pleistocene de Karpathos (Greece); mouvements verticaux et datations radiometriques. L'Anthropologie 88, 49–61.

Keraudren, B., Sorel, D., 1987. The terraces of Corinth (Greece)—A detailed record of eustatic sea-level variations during the last 500,000 years. Marine Geology 77, 99–107.

Kokkalas, S., Doutsos, T., in press. Strain partitioning along the south Hellenides (Eastern Crete, Greece). In: Panayides, I., Xenophontos, C. (Eds.), Third International Conference on the geology of the Eastern Mediterranean. Geological Survey Department, Cyprus.

Kontopoulos, N., Zelilidis, A., Frydas, D., 1996. Late Neogene sedimentary and tectonostratigraphic evolution of northwestern Crete island, Greece. Neues Jahrbuch fur Geologie und Palaontologie Abhandlungen 202, 287–311.

Koufos, G.D., Kostopoulos, D.S., Koliadimou, K.K., 1991. Une nouveau gisement de mammiferes dans le Villafranchien de Macedoine occidentale (Greece). Comptes Rendus de l'Academie des Sciences, Paris 313, 831–836.

Koukouvelas, I., Asimakopoulos, M., Doutsos, T., 1999. Fractal characteristics of active normal faults: an example of the eastern Gulf of Corinth, Greece. Tectonophysics 308, 263–274.

Koukouvelas, I., Mpresiakas, A., Sokos, E., Doutsos, T., 1996. The tectonic setting and earthquake ground hazards of the 1993 Pyrgos earthquake, Peloponnese, Greece. Journal of the Geological Society, London 153, 39–49.

Kowalczyk, G., Richter, D., Risch, H., Winter, K.P., 1977. Zur zeitlichen Einstufung der tektogenetischen Ereignisse auf dem Peloponnes (Griechenland). Neus Jahrbuch fur Geologie und Palaontologie Monatshefte 9, 549–564.

Kowalczyk, G., Winter, K.P., 1979. Die geologische Entwicklung der Kyllini-Halbinsel im Neogen und Quartar (West-Peloponnes, Griechenland). Zeitschrift der Deutschen Geologischen Gesellschaft 130, 323–346.

Ktenas, C.A., 1969. La geologie de l'ile de Nikaria. Geol. Geophys. Res. 13, 58–86.

Laj, C., Jamet, M., Sorel, D., Valente, J.P., 1982. First paleomagnetic results from Mio-Pliocene series of the Hellenic sedimentary arc. Tectonophysics 86, 45–67.

Le Pichon, X., Angelier, J., 1979. The Hellenic Arc and Trench system: a key to the Neotectonic evolution of the eastern Mediterranean area. Tectonophysics 60, 1–42.

Le Pichon, X., Angelier, J., Boulin, J., Bureau, D., Cadet, J.P., Chapel, A., Dercourt, J., Glacon, G., Got, H., Karig, D., Lyberis, N., Mascle, J., Ricou, L.E., Thiebault, F., 1980. Importance des formations attribuees au Messinien dans les fosses de subduction helleniques: observations par submersible. Comptes Rendus de l'Academie des Sciences, Paris 290, 5–8.

Le Pichon, X., Chamot-Rooke, N., Lallemant, S., Noomen, R., Veis, G., 1995. Geodetic determination of the kinematics of central Greece with respect to Europe: Implications for eastern Mediterranean tectonics. Journal of Geophysical Research 100, 12675–12690.

Leydecker, G., Berckhemer, H., Delibassis, N., 1978. A study of seismicity in the Peloponnese region by precice hypocenter determinations. In: Closs, H., Roeder, D., Schmidt, K. (Eds.), Alps, Appenines, Hellenides. Verlagbuchandlung, Stuttgart, pp. 406–410.

Louvari, E., Kiratzi, A.A., Papazachos, B.C., 1999. The Cephalonia Transform Fault and its extension to western Lefkada Island (Greece). Tectonophysics 308, 223–236.

Lyberis, E., Papatheodorou, G., Hasiotis, T., Ferentinos, G., 1998. Submarine faults within the active tectonic graben of the Gulf of Corinth. Four typical examples of modern tectonic control on morphology and sedimentation processes under the sea-level. Bulletin of the Geological Society of Greece 32, 223–234.

Lyberis, N., Angelier, J., Barrier, E., Lallemant, S., 1982. Active deformation of a segment of arc: the strait of Kythira, Hellenic arc, Greece. Journal of Structural Geology 4, 299–311.

Lyberis, N., Lallemant, S., 1985. La transition subduction-collision le long de l'arc egeen externe. Comptes Rendus de l'Academie des Sciences, Series II 300, 887–890.

Lyon-Caen, H., Armijo, R., Drakopoulos, J., Baskoutas, J., Delibasis, N., Gaulon, R., Kouskouna, V., Latoussakis, J., Makropoulos, K., Papadimitriou, P., Papanastasiou, D., Pedotti, G., 1988. The 1986 Kalamata (South Peloponnesus) earthquake: Detailed study of a normal fault, evidences for east-west extension in the Hellenic Arc. Journal of Geophysical Research 93, 14967–15000.

Maerten, L., Willemse, E.J.M., Pollard, D.D., Rawnsley, K., 1999. Slip distributions on intersecting normal faults. Journal of Structural Geology 21, 259–271.

Makris, J., 1978. Aegean crust and upper mantle. In: Closs, H., Roeder, D., Schmidt, K. (Eds.), Alps, Appenines, Hellenides. Verlagbuchandlung, Stuttgart, pp. 392–401.

Makris, J., Stobbe, C., 1984. Physical properties and state of the crust and upper mantle of the Eastern Mediterranean Sea deduced from geophysical data. Marine Geology 55, 347–363.

Marrett, R., Allmendinger, R.W., 1990. Kinematic analysis of fault-slip data. Journal of Structural Geology 12, 973–986.

Martin, L., Mascle, J., 1989. Structure et evolution recente de la mer Egee: II. Le domaine egeen central. Comptes Rendus de l'Academie des Sciences, Paris 309, 1487–1493.

Mascle, J., Le Quellec, P., Leite, O., Jongsma, D., 1982. Structural sketch of the Hellenic continental margin between the western Peloponnesus and eastern Crete. Geology 10, 113–116.

Mascle, J., Martin, L., 1990. Shallow structure and recent evolution of the Aegean Sea: A synthesis based on continuous reflection profiles. Marine Geology 94, 271–299.

McKenzie, D., 1972. Active tectonics of the Mediterranean region. Geophysical Journal of the Royal Astronomical Society 30, 109–182.

McKenzie, D., 1978. Active tectonics of the Alpine-Himalayan belt: the Aegean Sea and surrounding regions. Geophysical Journal of the Royal Astronomical Society 55, 217–254.

Meijer, P.T., Wortel, M.J.R., 1997. Present-day dynamics of the Aegean region: A model analysis of the horizontal pattern of stress and deformation. Tectonics 16, 879–895.

Melentis, J., Schneider, H., 1966. Eine neue Pikermifauna in der nahe der Ortschaft Alifaka in Thessalien. Annales Geologiques des Pays Helleniques 17, 267–288.

Mercier, J.L., Bousqet, B., Delibassis, N., Drakopoulos, I., Keraudren, B., Lemelle, F., Sorel, D., 1972. Deformations en compression dans le quaternaire de rivages ioniens (Cephalonie, Greece). Donnes neotectoniques et seismiques. Comptes Rendus de l'Akademie des Sciences 275, 2307–2310.

Mercier, J.L., Sorel, D., Vergely, P., Simeakis, K., 1989. Extensional tectonic regimes in the Aegean basins during the Cenozoic. Basin Research 2, 49–71.

Meulenkamp, J., Theodoropoulos, P., Tsapralis, V., 1977. Remarks on the Neogene of Kythira, Greece. VI Colloqium on the Geology of the Aegean Region 1, 355–362.

Meulenkamp, J., Wortel, M.J.R., Van Wamel, W.A., Spakman, W., Hoogerduyn Strating, E., 1988. On the Hellenic subduction zone and the geodynamic evolution of Crete since the late Middle Miocene. Tectonophysics 146, 203–215.

Mutti, E., Orombelli, G., Pozzi, R., 1970. Geological studies of the Dodecanese Islands (Aegean Sea)-Geological map of the Island of Rhodes and explanatory notes. Annales Geologiques des Pays Helleniques 22, 77–226.

Papazachos, B.C., Kiratzi, A., 1996. A detailed study of the active crustal

deformation in the Aegean and surrounding area. Tectonophysics 253, 129–154.

Papazachos, B.C., Karakostas, B., Scordilis, E., 1995. Space and time distribution of the 1995 seismic sequence in the Kozani-Grevena area. Abstracts of proceedings, In: International meeting on the results of the May 13, 1995 Kozani-Grevena earthquake: one year after. Technical Education Institute of Kozani, pp. 111-113.

Papazachos, B.C., Karakostas, V.G., Papazachos, C.B., Scordilis, E.M., 2000. The geometry of the Wadati-Benioff zone and lithospheric kinematics in the Hellenic arc. Tectonophysics 319, 275–300.

Papazachos, B.C., Kiratzi, A., Hatzidimitriou, P., Rocca, A., 1984. Seismic faults in the Aegean area. Tectonophysics 106, 71–85.

Papp, A., Steininger, F., 1979. The Pliocene of the Megara-Graben. In: Symeonidis, N. (Ed.), Field guide to the Neogene of Megara, Peloponnese and Zakynthos. Special Publications of the Geological Institute of Athens 31, pp. 3–16.

Pavlides, S., Mountrakis, D., 1987. Extensional tectonics of northwestern Macedonia, Greece, since the late Miocene. Journal of Structural Geology 9, 385–392.

Pavlides, S., Zouros, N., Chatzipetros, A., Kostopoulos, D., Mountrakis, D., 1995. The 13 May 1995 Western Macedonia, Greece (Kozani-Grevena) earthquake; preliminary results. Terra Nova 7, 544–549.

Petit, J.P., 1987. Criteria for the sense of movement on fault surfaces in brittle rocks. Journal of Structural Geology 9, 597–608.

Poulimenos, G., Doutsos, T., 1996. Barriers on seismogenic faults in central Greece. Journal of Geodynamics 22, 119–135.

Poulimenos, G., Albers, G., Doutsos, T., 1989. Neotectonic evolution of the central section of the Corinth graben. Zeitschrift der Deutschen Geologischen Gesellschaft 14, 273–282.

Price, S.P., Scott, B., 1994. Fault-block rotations at the edge of a zone of continental extension; southwest Turkey. Journal of Structural Geology 16, 381–392.

Reches, Z., 1987. Determination of the tectonic stress tensor from slip along faults that obey the Coulomb yield condition. Tectonics 6, 849–861.

Reinecke, T., Altherr, R., Hartung, B., Hatzipanagiotou, K., Kreuzer, H., Harre, W., Klein, H., Keller, J., Geenen, E., Boger, H., 1982. Remnants of late Cretaceous high temperature belt on the island of Anafi (Cyclades, Greece). Neus Jahrbuch fur Mineralogie Abhandlungen 145, 157–182.

Reuther, C.D., Ben-Avraham, Z., Grasso, M., 1993. Origin and the role of major strike-slip transfers during plate collision in the Central Mediterranean. Terra Nova 5, 249–257.

Roberts, G.P., 1996. Variation in fault-slip directions along active and segmented normal fault systems. Journal of Structural Geology 18, 835–845.

Roberts, G.P., Ganas, A. (in press). Fault-slip directions in central-southern Greece measured from striated and corrugated fault planes: comparison with focal mechanism and geodetic data. Journal of Geophysical Research.

Roberts, G.P., Koukouvelas, I., 1996. Structural and seismological segmentation of the Gulf of Corinth fault system: Implications for models of fault growth. Annali di Geofisica 39, 619–646.

Roesler, G., 1978. Relics of non-metamorphic sediments on Central Aegean islands. In: Closs, H., Roeder, D., Schmidt, K. (Eds.), Alps, Appenines, Hellenides. Verlagbuchandlung, Stuttgart, pp. 480–481.

Schneider, H., 1972. Beobactungen zum kontinentalen Neogen Thessaliens. Neus Jahrbuch fur Geologie und Palaontologie Monatshefte 3, 183–195.

Schneider, H., Velitzelos, E., 1973. Jungtertiare Pflanzenfunde aus dem Becken von Vegora in West-Mazedonien (Greichenland). Erste Mitteilung, Ann. Museum Goulandris 1, 245–249.

Scott, D.L., Braun, J., Etheridge, M.A., 1994. Dip analysis as a tool for estimating regional kinematics in extensional terranes. Journal of Structural Geology 16, 393–401.

Sengor, A.M.C., 1987. Cross-faults and differential stretching of hanging walls in regions of low-angle normal faulting: examples from western Turkey. In: Coward, M.P., Dewey, J.F., Hancock, P.L. (Eds.), Continental Extensional Tectonics. Geological Society Special Publication 28, pp. 575–579.

Smith, P.E., York, D., Chen, Y., Evensen, N.M., 1995. The timing of an ancient Greek paroxysm on the island of Kos: towards a more precise calibration of the Mediterranean Deep-Sea Record. American Geophysical Union, December 1995, fall meeting, Abstracts, F 712.

Spang, J.H., 1972. Numerical method for dynamic analysis of calcite twin lamellae. Geological Society of America Bulletin 83, 467–472.

Stewart, I., Vita-Finzi, C., 1996. Coastal uplift on active normal faults: The Eliki Fault, Greece. Geophysical Research Letters 23, 1853–1856.

Sylvester, A.G., 1988. Strike-slip faults. Geological Society of America Bulletin 100, 1666–1703.

Taymaz, T., Jackson, J., McKenzie, D., 1991. Active tectonics of the north and central Aegean Sea. Geophysical Journal International 106, 433–490.

Ten Veen, J.H., Postma, G., 1999. Neogene tectonics and basin fill patterns in the Hellenic outer-arc (Crete, Greece). Basin Research 11, 223–241.

Theodoropoulos, D., 1979. Samos Island, Geological Map 1:50000, with explanations. Institute of Geological and Mineral Exploration, Athens.

Tikoff, B., Wojtal, S.F., 1999. Displacement control of geologic structures. Journal of Structural Geology 21, 959–967.

Turner, F.J., 1953. Nature and dynamic interpretation of deformation lamellae in calcite of three marbles. American Journal of Science 251, 276–298.

Underhill, J.R., 1989. Late Cenozoic deformation of the Hellenide foreland, western Greece. Geological Society of America Bulletin 101, 613–634.

Van de Weerd, A., 1979. Early Ruscinian rodents and lagomorphs (Mammalia) from the lignites near Ptolemais (Macedonia, Greece). Proc. Koninklijke Nederlandse Akademie van Wetenschappen B82, 127–170.

Westaway, R., 1993. Neogene evolution of the Denizli region of western Turkey. Journal of Structural Geology 15, 37–53.

Westaway, R., 1994. Evidence for dynamic coupling of surface processes with isostatic compensation in the lower crust during active extension of western Turkey. Journal of Geophysical Research 99, 20203–20223.

Zelilidis, A., Doutsos, T., 1992. An interference pattern of Neotectonic faults in the Southwestern part of the Hellenic Forearc basin, Greece. Zeitschrift der Deutschen Geologischen Gesellschaft 143, 95–105.

Zoback, D., Zoback, M.L., 1991. Tectonic stress field of North America and relative plate motions. In: Slemmons, D.B., Engdahl, E.R., Zoback, M.D., Blackwell, D.D. (Eds.), Neotectonics of North America: Boulder, Colorado. Geological Society of America, pp. 339–366.